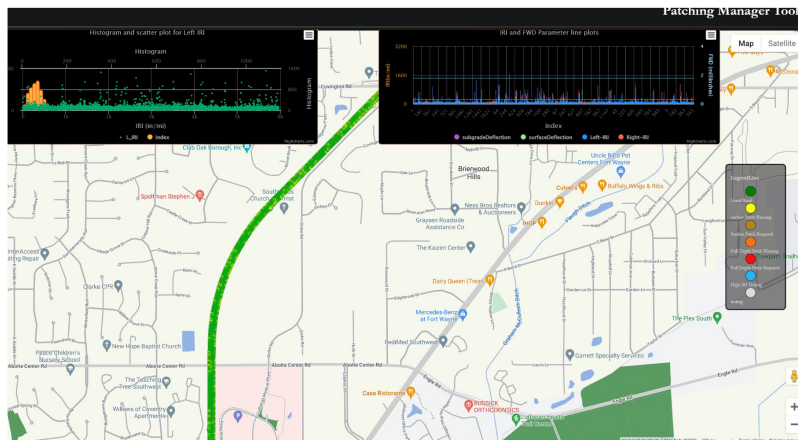
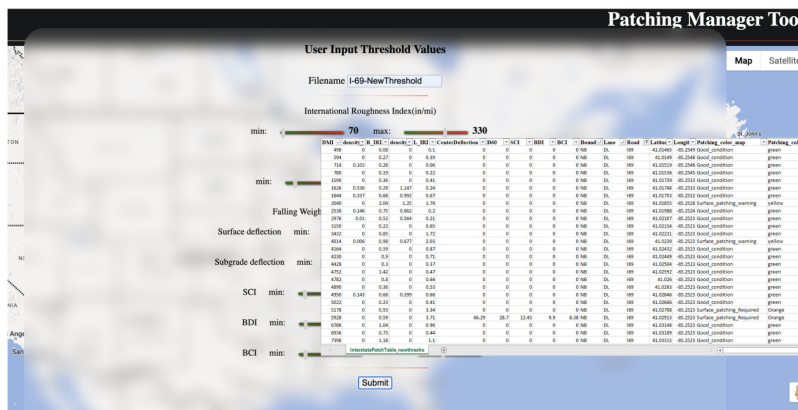




# Comprehensive Pavement Patching Tools and Web-Based Software for Pavement Condition Assessment and Visualization



(a)



**Sneha Jha, Yaguang Zhang, Tandra Bagchi, Andrew Balmos, Bongsuk Park, John E. Haddock, Seonghwan Cho, James V. Krogmeier**

## RECOMMENDED CITATION

Jha, S., Zhang, Y., Bagchi, T., Balmos, A., Park, B., Haddock, J. E., Cho, S., & Krogmeier, J. V. (2024). *Comprehensive pavement patching tools and web-based software for pavement condition assessment and visualization* (Joint Transportation Research Program Publication No. FHWA/IN/JTRP-2024/29). West Lafayette, IN: Purdue University. <https://doi.org/10.5703/1288284317770>

## AUTHORS

### **Sneha Jha**

Graduate Research Assistant  
Department of Agriculture and Biological Engineering,  
Purdue University

### **Yaguang Zhang, PhD**

Post-Doctoral Research Assistant  
School of Electrical and Computer Engineering  
Purdue University

### **Tandra Bagchi**

Graduate Research Assistant  
Lyles School of Civil Engineering  
Purdue University

### **Andrew Balmos**

Graduate Research Assistant  
School of Electrical and Computer Engineering  
Purdue University

### **Bongsuk Park, PhD**

Post-Doctoral Research Assistant  
Lyles School of Civil Engineering  
Purdue University

### **John E. Haddock, PhD**

Professor at Lyles School of Civil Engineering  
Purdue University

### **Seonghwan Cho, PhD**

Pavement Research Engineer  
Indiana Department of Transportation

### **James V. Krogmeier, PhD**

Professor of Electrical and Computer Engineering  
Elmore School of Electrical and Computer Engineering  
Purdue University  
(765) 494-3530  
[jvk@purdue.edu](mailto:jvk@purdue.edu)  
*Corresponding Author*

## JOINT TRANSPORTATION RESEARCH PROGRAM

The Joint Transportation Research Program serves as a vehicle for INDOT collaboration with higher education institutions and industry in Indiana to facilitate innovation that results in continuous improvement in the planning, design, construction, operation, management and economic efficiency of the Indiana transportation infrastructure. [https://engineering.purdue.edu/JTRP/index\\_html](https://engineering.purdue.edu/JTRP/index_html)

Published reports of the Joint Transportation Research Program are available at <http://docs.lib.purdue.edu/jtrp/>.

## NOTICE

The contents of this report reflect the views of the authors, who are responsible for the facts and the accuracy of the data presented herein. The contents do not necessarily reflect the official views and policies of the Indiana Department of Transportation or the Federal Highway Administration. The report does not constitute a standard, specification or regulation.

# TECHNICAL REPORT DOCUMENTATION PAGE

<b>1. Report No.</b> FHWA/IN/JTRP-2024/29	<b>2. Government Accession No.</b>	<b>3. Recipient's Catalog No.</b>	
<b>4. Title and Subtitle</b> Comprehensive Pavement Patching Tools and Web-Based Software for Pavement Condition Assessment and Visualization		<b>5. Report Date</b> September 2024	
		<b>6. Performing Organization Code</b>	
<b>7. Author(s)</b> Sneha Jha, Yaguang Zhang, Tandra Bagchi, Andrew Balmos, Bongsuk Park, John E. Haddock, Seonghwan Cho, and James V. Krogmeier		<b>8. Performing Organization Report No.</b> FHWA/IN/JTRP-2024/29	
<b>9. Performing Organization Name and Address</b> Joint Transportation Research Program Hall for Discovery and Learning Research (DLR), Suite 204 207 S. Martin Jischke Drive West Lafayette, IN 47907		<b>10. Work Unit No.</b>	
		<b>11. Contract or Grant No.</b> SPR-4521	
<b>12. Sponsoring Agency Name and Address</b> Indiana Department of Transportation (SPR) State Office Building 100 North Senate Avenue Indianapolis, IN 46204		<b>13. Type of Report and Period Covered</b> Final Report	
		<b>14. Sponsoring Agency Code</b>	
<b>15. Supplementary Notes</b> Conducted in cooperation with the U.S. Department of Transportation, Federal Highway Administration.			
<b>16. Abstract</b> <p>It is a common practice among state agencies to manually inspect road segments and decide maintenance requirements based on the pavement condition index (PCI). However, standalone PCI only evaluates the pavement surface condition. When coupled with the variability in human perception of pavement distress, this limits the accuracy of current pavement maintenance practices and undermines the automated pavement maintenance suggestions systems, especially for actionable recommendations related to accurate patching location, depth, and priority. This project explores integrating pavement structural and surface condition assessment with pavement ratings of distress to estimate the appropriate pavement patching strategy for accurate location, depth, and quantity. The developed patching management tool will provide an automated pavement management option with high resolution patching location and improved patching depth and priority suggestions.</p>			
<b>17. Key Words</b> pavement maintenance, patching management tool (PMT), pavement condition index (PCI), falling weight deflectometer (FWD), international roughness index (IRI), crack density, automated pavement assessment, geospatial data fusion, web-based application, pavement distress detection, structural number ratio (SNR), patching tables, eCDF, pavement types		<b>18. Distribution Statement</b> No restrictions. This document is available through the National Technical Information Service, Springfield, VA 22161.	
<b>19. Security Classif. (of this report)</b> Unclassified	<b>20. Security Classif. (of this page)</b> Unclassified	<b>21. No. of Pages</b> 42 including appendices	<b>22. Price</b>

## EXECUTIVE SUMMARY

### Motivation

It is a common practice among state agencies to manually inspect road segments that are of interest and decide on maintenance requirements based on the pavement condition index (PCI). However, standalone PCI only evaluates the pavement surface condition. When coupled with the variability in human perception of pavement distress, PCI limits the accuracy of current pavement maintenance practices, and undermines the automated pavement maintenance suggestions systems, especially when suggesting actionable recommendations for accurate patching location, depth, and priority. This project explored integrating pavement structural and surface condition assessments with pavement ratings of distress to estimate the appropriate pavement patching strategy using accurate location, depth, and quantity.

### Study

In this project, we looked at pavement structural condition parameters, falling weight deflectometer deflections with surface condition parameters, international roughness index, and cracking density for a better representation of overall pavement distress. A pavement-specific, threshold-based patching suggestion algorithm was designed to suggest pavement maintenance operations. The PCI thresholds for the developed algorithm were the intersecting values between the empirical cumulative distribution function for surface deflection and the structural number ratio threshold values for each pavement type. A web-based patching manager tool (PMT) was designed as an interactive tool to visualize and analyze pavement distress and patching suggestions on maps. The PMT was validated with road surface and right-of-way images obtained from three-dimensional laser sensors, which could successfully capture localized distresses in existing pavements. Finally, an implementation phase was conducted with two major outputs: (1) tooling was created to permanently store project data in an INDOT-managed Oracle database, and (2) the functionality of PMT was re-developed within an INDOT ArcGIS Online environment.

### Results

1. This study proposed a reliability-structural number ratio (SNR)-based threshold calculation method for integrated pavement condition assessment (PCA) parameters. The data fusion approach integrated structural and functional assessment parameters with the matched geographical location to

describe the overall pavement assessment with increased accuracy. It considered roughness, cracking and falling weight deflectometer (FWD) deflections at the same location and allowed for the automation of improved patching suggestions.

2. The patching suggestion algorithm incorporated the overall pavement condition information and created five pavement condition ratings based on the distress level in three major layers of the pavement structure. The algorithm was tested using calculated PCA parameter threshold values for interstate full-depth asphalt pavement segments. Comparative analysis of PCA parameters detected localized distresses, which may reduce the bulk human resource and time required in a manual routine survey.
3. Appropriate threshold values based on current road conditions were determined by comparing the cumulative distribution function of PCA parameters. This approach could be extended for any pavement type.
4. The developed threshold-based patching suggestion algorithm was reinforced with a web-based application, PMT, to assist in the current practices of pavement management system (PMS). The PMT web-based application provided high-resolution comprehensive patching suggestions, and it was successfully verified with right-of-way (ROW) images and Google Street View. Its key features are summarized below.
  - The web-application plotted comprehensive patching suggestions with color-coded markers for a selected road segment on a map.
  - PMT integrated two-dimensional road surface and ROW images to aid visual field assessments.
  - PMT allowed users to take advantage of Google Street View at the patching locations for 3D virtual spatial analysis.
  - Histogram and scatter plots were included to analyze the distribution or pattern in PCA parameters along/among the selected roads.
  - PMT supported the manual adjustment of threshold values for each PCA parameter in the patching suggestion algorithm. This feature created flexibility for users to customize the patching tables, which are essential for analyzing and updating maintenance standards.
5. Consequently, the PMT web-based application, along with the proposed approach for threshold determination could be applied to any region with different road conditions.
6. Project data was permanently stored in an INDOT-managed Oracle database. Tools were created to re-process and update stored as needed for improved thresholds.
7. The PMT functionality was developed within the INDOT ArcGIS Online environment.



## CONTENTS

1. PROJECT OVERVIEW .....	1
1.1 Introduction .....	1
1.2 Overview of PMT .....	1
2. REVIEW LITERATURE ON PAVEMENT PATCHING TECHNIQUES .....	4
2.1 Pavement Distress and Patching Methods .....	4
2.2 Patching Methods Implemented by DOTs .....	6
3. PAVEMENT CONDITION PARAMETER SELECTION .....	8
3.1 IRI and Crack Density .....	8
3.2 FWD .....	9
3.3 TSD .....	10
3.4 GPR .....	10
4. GEOSPATIAL DATA FUSION OF PCI PARAMETERS .....	10
4.1 Geospatial Data Fusion .....	10
4.2 Evaluation of the Fused Data .....	11
5. THRESHOLD CALCULATION AND PATCHING SUGGESTION ALGORITHM .....	13
5.1 Determination of FWD Parameters Thresholds .....	13
5.2 Determination of Preliminary FWD Thresholds Using Reliability .....	13
5.3 Verification of FWD Thresholds Using the Structural Number Ratio (SNR) .....	15
5.4 Determination of Functional Parameters Thresholds .....	16
5.5 Evaluation of Geo-Indexed Data Using Calculated Threshold Values .....	16
5.6 Patching Suggestion Algorithm .....	17
6. PMT WEB-APPLICATION .....	21
6.1 Current Database .....	21
6.2 Geospatial Data Processing .....	21
6.3 Patching Management Tool .....	21
6.4 PMT Web-Application Design .....	22
7. INDOT IMPLEMENTATION .....	24
7.1 Data Sources .....	24
7.2 Data Processing .....	24
7.3 ArcGIS Online Feature Layer .....	27
7.4 ArcGIS Dashboard .....	27
8. FUTURE WORK .....	30
9. RESULTS SUMMARY AND RECOMMENDATIONS .....	30
9.1 Results Summary .....	30
9.2 Recommendations .....	30
REFERENCES .....	30
APPENDICES	
Appendix A. Processing of Raw 3D Laser Data in Waylink's ADA3 Software .....	33

## LIST OF TABLES

<b>Table 5.1</b> Reliability Results of FWD Deflection Parameters	15
<b>Table 5.2</b> Final Threshold Values of FWD Deflection Parameters	18
<b>Table 5.3</b> Threshold-Based Patching Suggestion Algorithm for Interstate Full-Depth Asphalt Pavement	20

## LIST OF FIGURES

<b>Figure 1.1</b> Displaying the center deflection ranges of eight sections of interstate roads in Indiana	2
<b>Figure 1.2</b> Patching suggestion displayed for selecting a single road section in PMT	2
<b>Figure 1.3</b> Street view of the selected location with surface patching warning	3
<b>Figure 1.4</b> An example patching suggestion table downloaded from the PMT. The background shows the window to input user threshold values	3
<b>Figure 2.1</b> Different types of asphalt pavement distresses	4
<b>Figure 2.2</b> Throw-and-roll procedure	5
<b>Figure 2.3</b> Semi-permanent method	5
<b>Figure 2.4</b> Spray injection method	6
<b>Figure 2.5</b> Edge sealing method	6
<b>Figure 2.6</b> Partial depth patching: (a) sawing, (b) removing, and (c) placing	7
<b>Figure 2.7</b> Full-depth patching: (a) removing the existing slab, (b) placing the subbase materials, (c–d) compacting the subbase, and (e) the new slab surface	7
<b>Figure 3.1</b> Location of geophones for FWD test	9
<b>Figure 4.1</b> Flow diagram of sensor data fusion	11
<b>Figure 4.2</b> Comparison of FWD deflection parameters from all road classifications	12
<b>Figure 4.3</b> IRI data from WayLink ADA3	12
<b>Figure 4.4</b> DMI with high IRI, FWD deflections, and CD identified (a) using stem plot, and (b) the ROW and road surface image for the identified DMI on I-70 from WayLink	13
<b>Figure 5.1</b> ECDF plot for FWD deflection parameters on interstate full-depth asphalt pavement: (a) center deflection (D0), (b) subgrade deflection (D60), (c) SCI, (d) BCI, and (e) BDI	14
<b>Figure 5.2</b> Comparison between SNR and D0: (a) state road, (b) U.S. highway, and (c) interstate highway	17
<b>Figure 5.3</b> ECDF plot for functional parameters of interstate highway: (a) IRI and (b) CD	18
<b>Figure 5.4</b> Comparison of IRI and FWD on I-70: (a) left IRI, (b) right IRI, (c) center deflection D0, and (d) subgrade deflection D60. The Y-axis ranges of (c) and (d) are different to conserve the necessary information in both figures	19
<b>Figure 5.5</b> Patching conditions labeled according to the measurement range of FWD deflections	20
<b>Figure 6.1</b> The data flow structure in the PMT web application	21
<b>Figure 6.2</b> The flow diagram of processing the raw data for the patching manager tool (PMT)	22
<b>Figure 6.3</b> Web-based patching manager tool: (a) patching suggestion for the example road I-69 using color coded markers and graphs for analyzing the parameters, and (b) user input threshold selector for patching suggestion calculation with an example patching table	23
<b>Figure 6.4</b> Example of the final output of patching suggestion in PMT	24
<b>Figure 7.1</b> Flowchart for processing raw measurement data through the SPR-4521 algorithm and into the INDOT preferred storage and visualization tools	25
<b>Figure 7.2</b> FME workflow to load CSV output and load into Oracle (rotated)	26
<b>Figure 7.3</b> FME workflow for transferring data stored in SPR-4521 Oracle tables into ArcGIS Online for visualization and custom analysis	27
<b>Figure 7.4</b> Default styling of SPR-4521 patching recommendations layered into a new ArcGIS project	28
<b>Figure 7.5</b> ArcGIS Online dashboard for the SPR-4521 hosted feature layer, designed to enable a more effective review of a recommended patching table	28
<b>Figure 7.6</b> Selecting points in the line graph visually filters the points in the map. This allows for quickly “zooming” into areas of interest based on abnormal measurement trends	29
<b>Figure 7.7</b> By selecting a small number of locations of interest, one can “click through” the set of ROW and surface images to explain and/or validate patching recommendations. In this case, the sudden spike of IRI can be accounted for by noticing that the road transitions from new to old, formerly patched pavement	29

## 1. PROJECT OVERVIEW

### 1.1 Introduction

According to the Federal Highway Administration, the United States has approximately 4 million miles of roads, making it one of the largest road networks in the world. Road networks are crucial to economic activities, with the transportation sector accounting for about 8.9% of the U.S. gross domestic product (GDP) in 2020. With increasing traffic loads, the maintenance of these roads has become a significant challenge. In Indiana alone, the Department of Transportation invests billions of public-funded dollars in maintaining about 11,000 centerline kilometers of roads. However, the implementation of maintenance strategies is limited due to the maintenance scale and the variability in human perception of pavement distress (Baladi et al., 2017; Chikezie et al., 2013; Haider et al., 2011). To address this challenge, there is an increasing demand for automated pavement maintenance systems that can cover large areas with better accuracy (Kulkarni & Miller, 2003; Wolters & Zimmerman, 2010).

### 1.2 Overview of PMT

A web-based comprehensive patching suggestion application, patching management tool (PMT) was developed by incorporating both functional and structural conditions of existing pavements into a threshold-based patching suggestion algorithm. It determines the threshold values of falling weight deflectometer (FWD), international roughness index (IRI), and crack density (CD) parameters from current pavement condition measurements for different road and pavement. Field data from 2016 to 2021 was used to determine appropriate threshold values for the patching suggestion algorithm in the current version of the PMT.

#### 1.2.1 Geospatial Data Fusion of PCI Parameters

Comprehensive pavement maintenance requires both surface and structural condition assessments. Thus, an information fusion of the surface and structural condition parameters is desirable to generate a comprehensive pavement condition assessment. Integrating the IRI, CD, and FWD measurement data spatially facilitates local distress detection and monitoring over all road structural condition using surface condition parameters and FWD DBP, respectively. The multi-sensor data fusion method for creating high-resolution patching suggestions, spatially integrates pavement condition assessment (PCA) parameters, IRI and CD, measured from the three-dimensional (3D) laser imaging sensor, with pavement deflection basin parameters measured by FWD. Ground penetrating radar (GPR) depth data was used to identify pavement types in FWD data processing.

#### 1.2.2 Patching Algorithm and Threshold Calculation

Thresholds of FWD parameters were preliminarily determined based on the concept of design reliability, which is the probability of good pavement sections over the design period. According to the *Mechanistic-Empirical Pavement Design Guide*, the reliability concept is recommended for determining performance threshold values to achieve a balance between maintenance costs and overall pavement structural health. Threshold values of pavement condition parameters were selected to define three levels of pavement conditions as good, fair, and poor. Conditional inequality was used to categorize the overall pavement condition metrics into five pavement condition ratings. Each condition marked the roads condition from severe road damage to good road and suggests a recommended pavement patching method. This suggestion includes the Patching length, width and depth. This algorithm provides the ability to prioritize the maintenance of the roads with worst current condition while minimizing manual perception error of faults.

#### 1.2.3 PMT Web Application

A web-based application can be hosted on an internet browser and hence is easily available to view with correct credentials. The open-source structure of the application also makes it free to use for individual analysts/engineers. In the PMT application, the threshold-based patching algorithm is currently implemented using the spatially indexed and integrated PCA parameters to create patching suggestions for roads of interest. The PMT also displays multiple roads across the whole state and uses the patching suggestion algorithm to compare road conditions over large area networks. Figure 1.1 shows the center deflection values across 8 roads sections in Indiana. The interactive feature of the PMT allows the user to select single road sections for zoom-in view of the road. It also displays the distribution of the PCA parameters on a selected road. The screen grab in Figure 1.2 shows the display of the PMT when a single road is selected. Figure 1.3 shows the 2D road surface and right-of-way (ROW) images for selected road section in PMT which makes it easier to scout for faults using image data near high PCA values or patching suggestions. If the user selects a specific location on the map the PMT uses the google Application Programming Interface (API) to display the street view at that location, including the patching table, as shown in Figure 1.4. The PMT also facilitates users to define threshold values to calculate patching suggestions and download patching suggestion tables in .csv format. The PMT provides the user with the ability to completely analyze the road conditions using images, PCA values and statistical analysis.

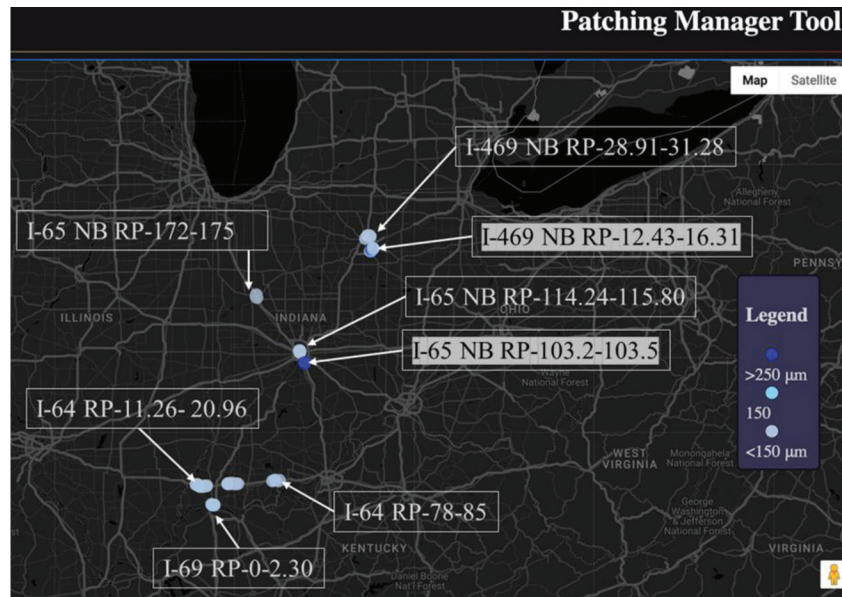


**Figure 1.1** Displaying the center deflection ranges of eight sections of interstate roads in Indiana.

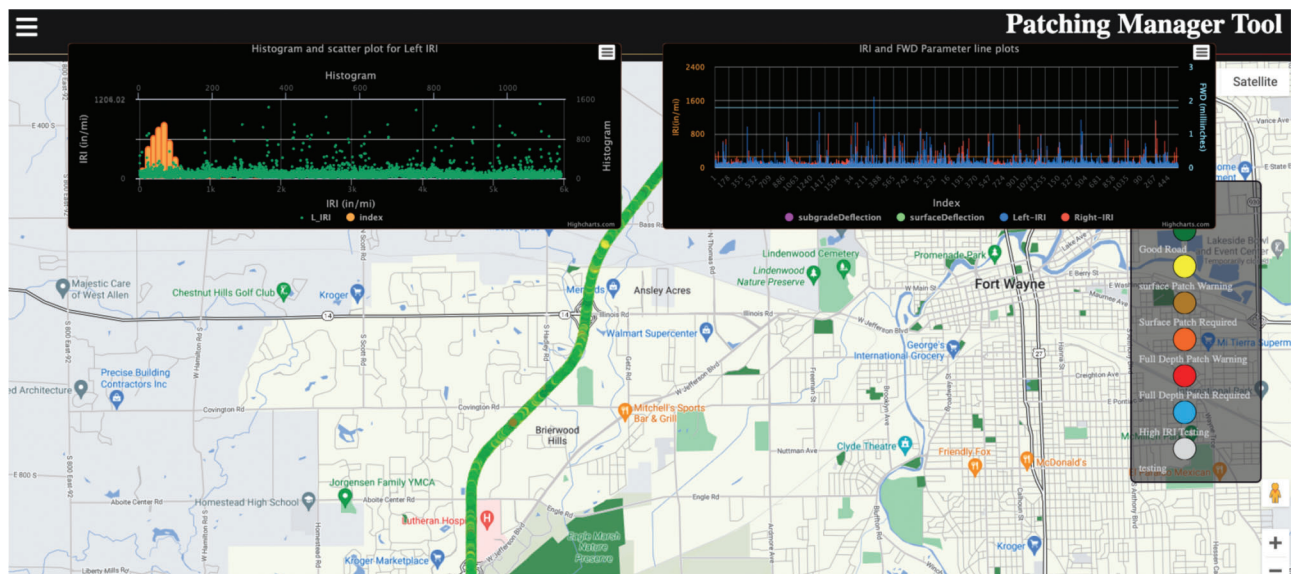


**Figure 1.2** Patching suggestion displayed for selecting a single road section in PMT.



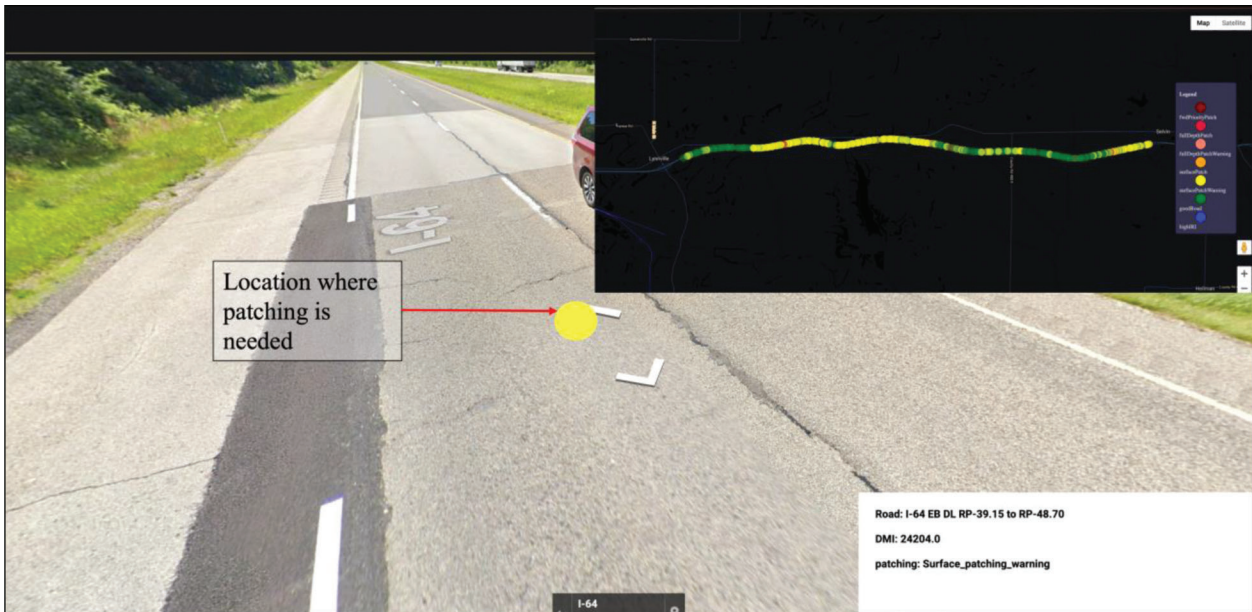


**Figure 1.3** Street view of the selected location with surface patching warning.

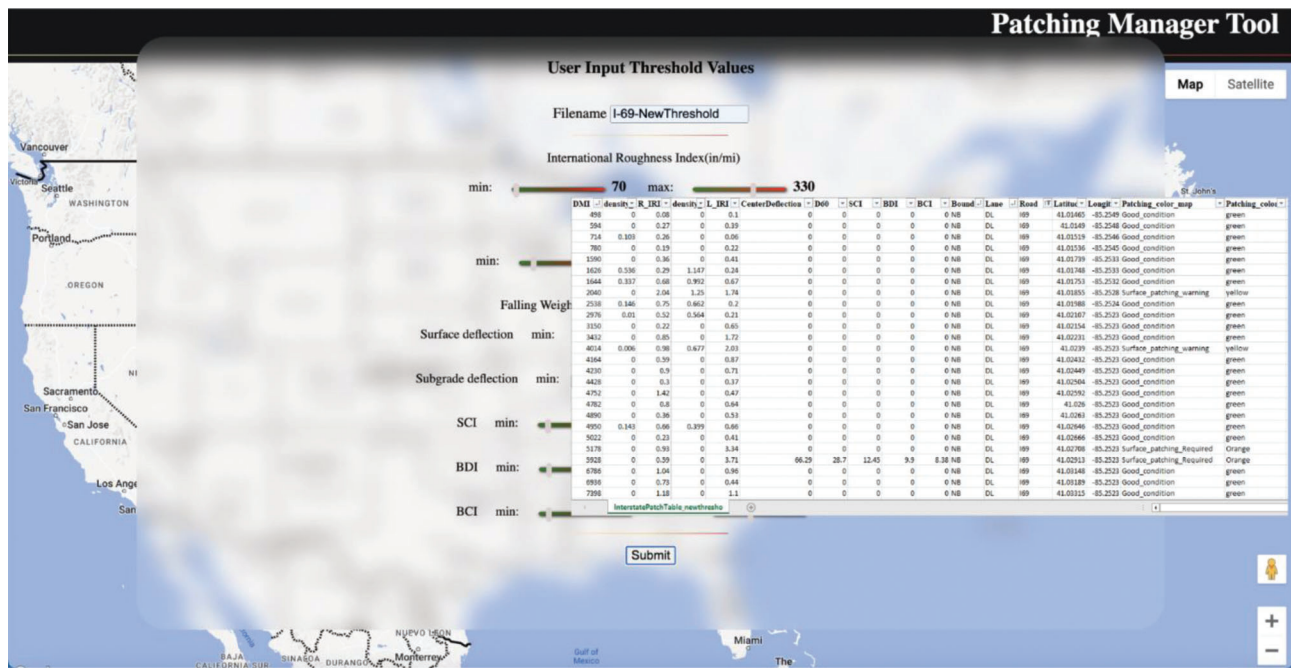


**Figure 1.4** An example patching suggestion table downloaded from the PMT. The background shows the window to input user threshold values.

## 2. REVIEW LITERATURE ON PAVEMENT PATCHING TECHNIQUES

Pavement patching is one of the most extensive and expensive pavement maintenance activities undertaken by highway agencies at all levels (AASHTO, 1993). Almost all U.S. states place great importance on pavement patching. The materials used for patching vary widely but fall into several general categories (Abd El-Raof et al., 2018). Asphalt materials are mostly used for temporary patching of both concrete and asphalt pavements (AASHTO, 1993). Permanent patches on concrete pavements are commonly made with cementitious materials of varying types, depending on the type of patch, type of roadway, and how long the patch can be allowed to cure or set. Epoxies and other polymeric materials are sometimes but less commonly used, because of the costs and complexity in handling and placement. On asphalt pavements, hot mix asphalt remains the preferred material for semi-permanent patching; however, the use of spray injection patching is increasing, and the performance is reportedly approaching semi-permanent status in some states. This success, however, has not been found in all states.

Indiana pavements are generally described as asphalt (flexible), concrete (rigid), or asphalt-over-concrete composites. Pavement patching or maintenance over INDOT's roughly 11,000 centerline-mile state network (Anderson & Thomas, 1984) is a significant expense year to year and pavement patching activities are a significant fraction of all pavement maintenance

activities. So, it is crucial to find out about the damaged roadway section as well as the extent of the damage before starting the maintenance work.

### 2.1 Pavement Distress and Patching Methods

Pavement distress is one of the main problems faced by DOTs. There are different kinds of distresses in both asphalt and concrete pavement, as shown in Figure 2.1. The common distresses of asphalt pavement are fatigue cracking, rutting, thermal cracking, water bleeding and pumping, stripping, raveling and so on. For concrete pavement the distresses are longitudinal cracking, faulting, curling, joint spalling and so on.

There are different pavement patching methods used by U.S. DOTs to repair damaged pavements. The common methods are given below.

#### 2.1.1 Throw-and-Roll

The steps of throw-and-roll method, depicted in Figure 2.2, is placing patch material into a pothole (which may or may not be filled with water or debris). Then, compacting the patch using truck tires. Verifying that the compacted patch has some crown (between 3 and 6 mm). After that, move on to the next pothole. And finally opening the repaired section to traffic as soon as maintenance workers and equipment are cleared from the area (Dong et al., 2013; Maher et al., 2001; McDaniel, 2020; Wilson & Romine, 2001).



**Figure 2.1** Different types of asphalt pavement distresses.





**Figure 2.2** Throw-and-roll procedure.

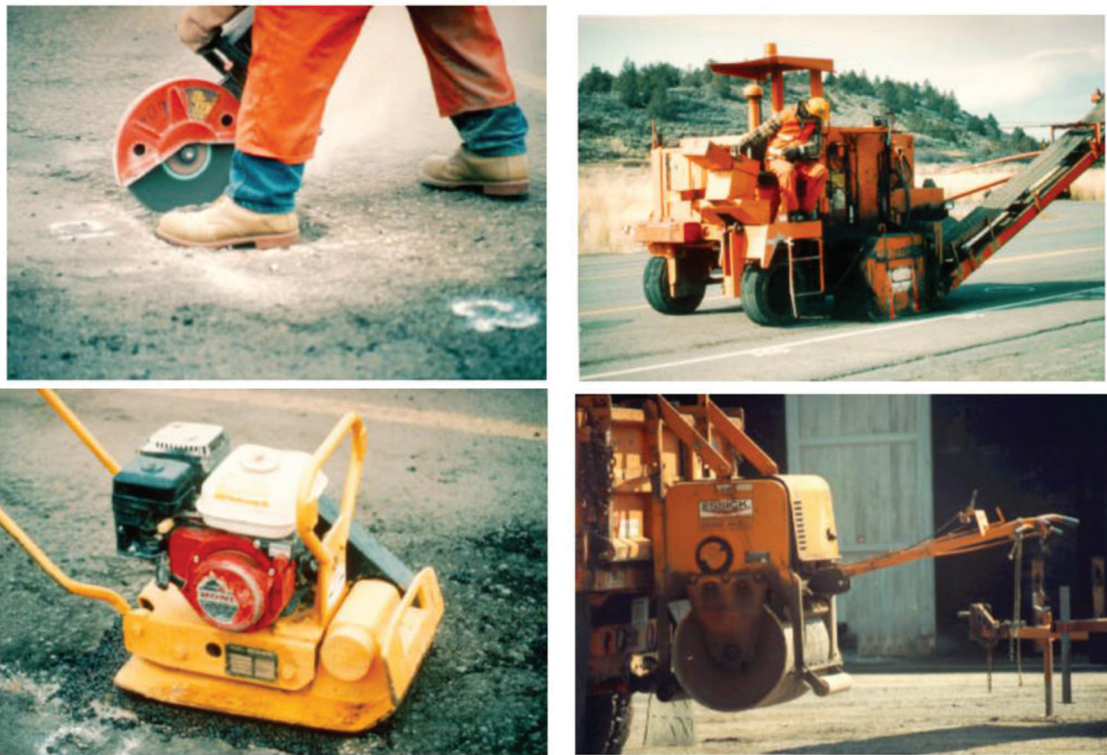


**Figure 2.3** Semi-permanent method.

### 2.1.2 Semi-Permanent

The semi-permanent repair method, depicted in Figure 2.3, is considered one of the best for repairing potholes, short of full-depth removal and replacement. This procedure includes the following steps: remove water and debris from the pothole. Square-up the sides of the patch area until vertical sides exist in reasonably sound pavement. Then placing the mix. Compact with a device smaller than the patch area (single-drum vibratory rollers and vibratory plate compactors work best). Finally, open the repaired section to traffic as soon as maintenance workers and equipment are cleared from the area (Dong et al.,

2013; Maher et al., 2001; McDaniel, 2020; Wilson & Romine, 2001).

### 2.1.3 Spray Injection

The spray-injection procedure, shown in Figure 2.4, consists of the following steps: Blow water and debris from the pothole. Spray a tack coat of binder on the sides and bottom of the pothole. Blow asphalt and aggregate into the pothole. Cover the patched area with a layer of aggregate. This procedure requires no compaction after the cover aggregate has been placed (Dong et al., 2013; Maher et al., 2001; McDaniel, 2020; Wilson & Romine, 2001).



**Figure 2.4** Spray injection method.



#### 2.1.4 Edge Seal

The edge seal method, imaged in Figure 2.5, consists of the following steps: Place the material into a pothole (which may or may not be filled with water or debris). Compact the patch using truck tires. Verify that the compacted patch has some crown (between 3 and 6 mm). Move on to the next pothole. Once the repaired section has dried, place a ribbon of asphaltic tack material on top of the patch edge (tack material should be placed on both patch and pavement surfaces). Place a layer of sand on the tack material to prevent tracking by vehicle tires. Open the repaired section to traffic as soon as maintenance workers and equipment are cleared from the area. This procedure may require a second visit to the repaired section by the crew to allow water to dry before placing the tack. Although this does reduce the productivity of the procedure, the placement of the tack material prevents water from getting through the edge of the patch and can glue together pieces of the surrounding pavement, improving support for the patch (Dong et al., 2013; Maher et al., 2001; McDaniel, 2020; Wilson & Romine, 2001).

### 2.2 Patching Methods Implemented by DOTs

For partial depth patching, as shown in Figure 2.6, starts with the small and shallow areas of deteriorated PCCP at distressed joints with rapid-setting patching materials were removed. Partial depth repairs must have a minimum dimension of 4 in. by 12 in. and 1 to 3 in. in depth. The partial depth patch should not be placed on frozen existing concrete pavements or under rainy conditions. For rapid-setting concrete filler, a non-vapor-barrier type bonding agent is applied to vertical and horizontal surfaces. Filler materials are slightly overfilled to allow counteracting for volume reduction during consolidation. PCCP filler is consolidated using vibrators. The patching area then leveled with the adjacent pavement and matched the texture of the patched surface to that of the existing pavement. Adequate attention is given to curing to reduce shrinkage cracking. Insulating blankets and



**Figure 2.5** Edge sealing method.

traps are used to reduce curing time. For HMA Filler, a bonding agent (AE-T) is applied to vertical and horizontal surfaces. Then the filler materials are slightly overfilled to allow counteracting for volume reduction during compaction. A vibratory roller with a minimum of four passes is used for compaction (Lee & Shields, 2010).

For full depth patching, featured in Figure 2.7, patch boundaries are identified and marked on the pavement surface based on engineering judgment using the data from coring, FWD testing, GPR testing, etc. A saw cut is made to the full lane width and depth over the marked length. The saw cut slab is broken into smaller pieces using a mechanical hammer or rammer and removed by backhoe. The disturbed base/subgrade is replaced, treated, or compacted. Filler materials are slightly overfilled to allow counteracting for volume reduction during consolidation. PCCP filler is consolidated using vibrators. The patching area then leveled with the adjacent pavement and matched the texture of the patched surface to that of the existing pavement. Adequate attention is given to curing to reduce shrinkage cracking. Insulating blankets and traps are used to reduce curing time (Lee & Shields, 2010).



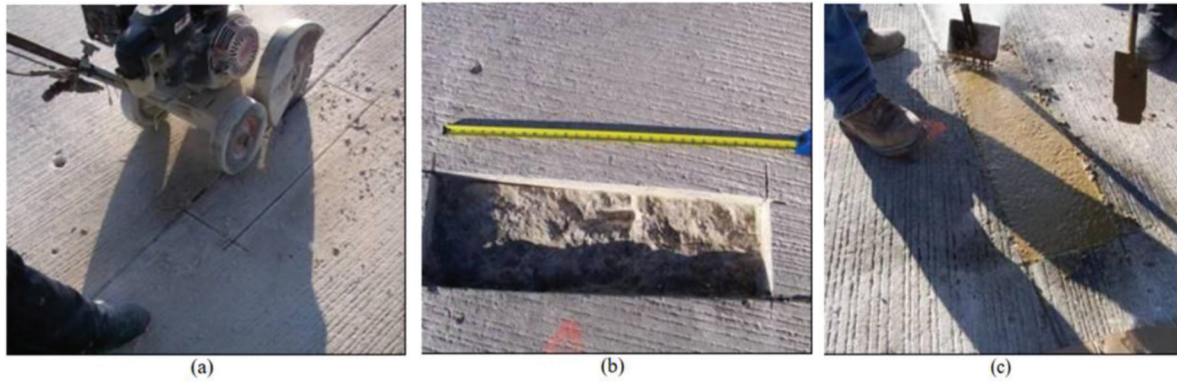


**Figure 2.6** Partial depth patching: (a) sawing, (b) removing, and (c) placing.



**Figure 2.7** Full-depth patching: (a) removing the existing slab, (b) placing the subbase materials, (c–d) compacting the subbase, and (e) the new slab surface.

### 2.2.1 Patching Techniques Implemented by MnDOT

Three steps are implemented to do the full depth permanent patching. The first step is to mark the area to be patched, extending outside the distressed area. The outline should be rectangular with two sides at right angles to the direction of traffic. Then cutting the outline of the patch with a saw, milling machine, or jackhammer. In the second step, excavation is done to remove as much pavement as necessary, including granular base and subgrade. The faces of the excavation should be straight, vertical, and solid. Trimming and compacting the granular base or subgrade is done to establish a firm foundation. A tack is applied to the vertical edges of the excavation, and a prime or tack coat to the base of the excavation. The third step is to backfill the excavation with asphalt mixture.

The patching mixture is shoveled directly from the truck and spread carefully to avoid segregation. After compaction, the surface of the patch should be at the same grade as the surrounding pavement (Johnson, 2000).

### 2.2.2 Patching Techniques Implemented by California DOT

For partial depth patching, the broken, damaged, or disintegrated concrete pavement is removed first. The limits of the damaged or defective areas should be determined by striking the pavement along the sides of each joint with a hammer or similar tool to detect concrete that sounds hollow.

The defective area is then marked by making a rectangle 2 in. beyond the outer limits of the unsound

concrete area as a guide for sawing. When the spalled joint is less than 6 in. long and 1.5 in. wide, thoroughly clean and reseal the joint. The rectangular marked areas are saw cut with near vertical faces at least 2 in. but no more than 3 in. deep. Unsound material is removed within the sawed area with a chipping hammer. Oil, dust, dirt, slurry and other contaminants caused by the sawing operation are removed. A 0.25-in.-wide piece of closed cell polyethylene foam shaped to fit the saw cut in the joints bordering the repair areas is placed and then patching materials are placed. Compaction is done as the same grade of existing pavement (Bautista & Basheer, 2008).

#### *2.2.3 Patching Techniques Implemented by TxDOT*

When the area is less than 6 in. in length and 1.5 in. in width, partial depth patch is considered. This treatment repairs localized distresses within the upper third to upper half slab thickness. The first step is to remove small shallow deteriorated areas by milling, chipping, and sawing of unsound concrete. Then the filler materials are placed. The filler can be rapid-setting concrete, conventional PCC, bituminous materials (based on curing time, climatic conditions, materials costs, and desired life). Partial depth repairs must have a minimum dimension of 4 in. by 12 in. and 1 to 3 in. in depth. The partial depth patch should not be placed on frozen existing concrete pavements or under rainy conditions (Chang et al., 2014)

#### *2.2.4 Patching Techniques Implemented by PennDOT*

The patching method uses cold stockpile patch material or hot mix and includes detailed procedures. First, marking defines the amount of material that should be removed. The cutting is done to remove weak and deteriorated material so that there will be firm material around the repair. After cutting is completed, the sides of the hold should be vertical. The hole does not have to be cut in the shape of a square. Often an L- or T-shaped cut is more effective. The cut is made with a series of straight lines. The cutting begins at the center of the hole and proceeds to the edges; the materials are broken and loosened as the cut is widened. Hydraulic, gas-operated, or air-operated cutting tools are used. The cut is deep enough to remove all loose and deteriorated material. Compressed air delivered from a blow pipe is the best cleaning method to clean the corners. The tack is used to “wet” the old pavement so that new patch material will stick or bond to it. The patch material is placed in even layers until there is sufficient material mounded above the surface of the pavement. It is very important that enough initial material be placed in the hole so that after final compaction, the surface of the patch is slightly above the pavement surface (Anderson & Thomas, 1984).

### **3. PAVEMENT CONDITION PARAMETER SELECTION**

Surface patching, thin overlay, and structural overlay are typical methods used for the preservation and rehabilitation of pavements. These techniques use either visual distress indicators or decision trees based on the pavement condition indices such as ride quality, pavement distress index etc. (Ismail et al., 2009; Kavussi et al., 2017; McDaniel et al., 2014). PCI includes the international roughness index (IRI), rut depth, and crack density (CD) to classify pavement surface conditions (Bryce et al., 2019; Setiাপutri et al., 2020; Sidess et al., 2021). Even though PCI is successful in characterizing pavement rideability, it does not properly account for the effect of pavement structural conditions.

The structural condition of the pavement is usually measured by the FWD and structural number index calculated from the FWD center deflection (Lytton, 1989; Rohde, 1994). However, the structural condition of the pavement is better represented by the DBPs, which reflect the layer condition at different depths in the pavement (Horak et al., 2015; Xiao et al., 2022).

Comprehensive pavement maintenance requires both surface and structural condition assessments. Thus, an information fusion of the surface and structural condition parameters is desirable to generate a comprehensive pavement condition assessment. Integrating the IRI, CD, and FWD measurement data spatially can allow both local distress detection and overall road structural condition using the high-resolution surface condition parameters and FWD DBPs, respectively. On these grounds, a complete patching suggestion based on a multi-sensor data fusion approach is proposed in this study.

#### **3.1 IRI and Crack Density**

The IRI and CD data used in this study were processed by commercial software, WayLink ADA3 (Wang et al., 2011, 2021). This software can recalculate IRI for selected spatial resolutions and match the results with the road surface images obtained from the 3D laser imaging sensor and right-of-way (ROW) images. In this study, a 6-ft. length along the road was selected as the spatial resolution. The WayLink ADA3 software uses an improved crack detection technique from 3D laser images using image processing and deep-learning neural networks (Zhang et al., 2017). The crack detection results provide a percentage of cracking on the left wheel path and right wheel path with the same spatial resolution as IRI.

##### *3.1.1 Processing IRI and CD Data*

The IRI raw data from the WayLink consists of raw data from multiple high-frequency laser sensors mounted on the front of the vehicle. The measurements are recorded at high resolution using distance measurement

instrument (DMI). The DMI is a self-contained, differential GPS (DGPS) receiver/antenna; and a solid-state, multi-axis, inertial sensing gyroscope, mounted on the driver's side rear wheel's axis-of-rotation to accurately represent the vehicle's movement, distance, and speed. The differential GPS receiver accepts RTCM-104 DGPS correction, suitable for some of the most extreme conditions. The receiver is mounted on top of the vehicle and has a refresh rate of 10 Hz. The multi-axis inertial sensing gyroscope contains three orthogonally mounted micro-machined quartz angular rate sensors and three silicon-based accelerometers for measuring linear accelerations and angular rates. The Automated Pavement Surface Imaging (APSI-4096) has a transverse resolution of 4,096 pixels, achieving 1-mm resolution with complete coverage of pavement surface at highway speed and is used to take pavement images for calculating cracking percentages.

These raw data are batch processed by the automated distress analyzer (ADA3) software filtering algorithms to clean noises from the signal and performs real-time IRI calculations according to the American Standards and Testing Materials consortium (ASTM) and crack maps, cracking classification, cracking percentage calculations using the AASHTO protocol. The processed files are also geo-indexed at each unit length of 6 ft. This project has WayLink's data for six interstate road sections of total length 89.49 miles, nine state roads of total length 45.09 miles and three U.S. highways of total length 18.28 miles.

### 3.1.2 Image Data from WayLink

The pavement right-of-way (ROW) images are high-definition 1,080p colored area-scan images taken from the top of the vehicle. These ROW and 2D/3D road surface images from APSI-4096 are also processed, resampled and geo-indexed by the ADA3 software at 6 ft. DMI. These processed high-resolution images constitute the major share of WayLink's data and occupy 3TB space on disc.

### 3.2 FWD

The falling weight deflectometer (FWD) is widely used as a non-destructive testing device for evaluating pavement structural conditions by measuring pavement surface deflections. The FWD is designed to simulate a single heavy truck wheel load by applying an impulse load to the pavement surface. Three impulse load levels (31 kN, 40 kN, and 49 kN) are used for one set of FWD loading. Nine geophones are placed longitudinally at various distances from the center of the FWD loading plate, as shown in Figure 3.1, to measure the pavement surface deflections, and  $D_x$  indicates the deflection measured at "x" distance from the FWD loading center. These measured deflections are typically used to obtain the FWD deflection basin curve and DBPs to provide more insights into the pavement structural capacity. It should be noted that for asphalt pavements, the maximum deflection ( $D_0$ ) was adjusted to the reference

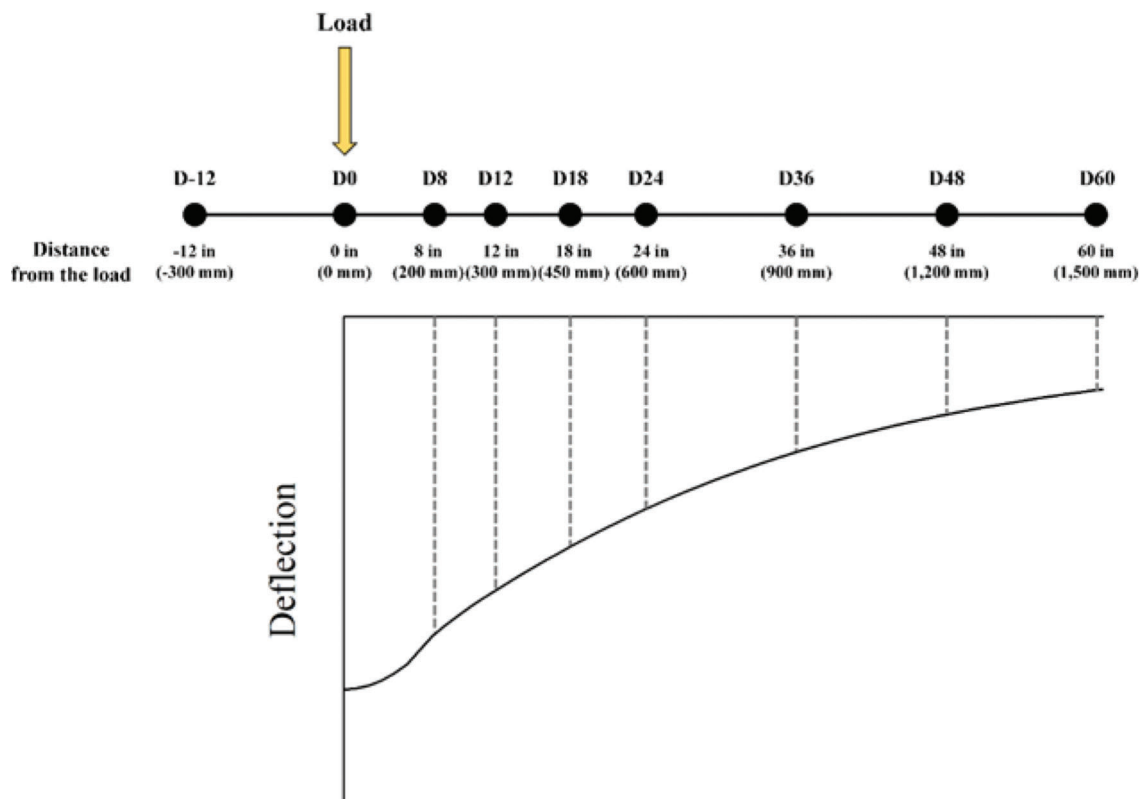


**Figure 3.1** Location of geophones for FWD test.



temperature (20°C) to eliminate the temperature effects, following the AASHTO 1993 method.

Two FWD deflection values (D0 and D60) and three DBPs were selected for this study to determine appropriate patching depth by interpreting structural conditions of specific pavement layers (Park et al., 2022). The D0 is used to evaluate overall pavement condition, while the D60, the deflection measured 1,500 mm (60 in.) from the center of loading plate, represents subgrade condition (Rohde, 1994). In addition, the FWD DBPs have been developed to assess the structural conditions of individual pavement layers, and three DBPs, including surface curvature index (SCI), base damage index (BDI), and base curvature index (BCI) were used for this (Gkyrtis et al., 2021; Lytton, 1989). The SCI is the difference of deflections measured from the center of the loading plate (D0) and 300 mm (12 in.) from the loading center (D12) to characterize the pavement upper layers conditions (16). The BDI is defined as a difference of D12, and the deflection measured 600 mm (24 in.) away from the loading center (D24), while BCI is the difference between D24 and D36 (deflection measured 900 mm away from the loading center). Both BDI and BCI have been developed to represent the conditions of base and subbase layers, respectively, and previous researchers have reported that BDI is mainly related to the aggregate base modulus, while BCI is more associated with the subgrade modulus (Horak et al., 2015; Sollazzo et al., 2017).

### 3.3 TSD

The traffic speed deflection devices (TSDDs) can assess the structural condition of pavements at network level. INDOT uses the traffic speed deflectometer (TSD) for its network level structural condition measurements. The TSD is an articulated truck with a rear-axle load that can be varied from 13.4 kips to 29.2 kips (60 kN to 130 kN) by using sealed lead loads. The TSD has up to a dozen Doppler lasers mounted on a servo-hydraulic beam to measure the deflection velocity of a loaded pavement. Doppler lasers are positioned to measure pavement deflection velocities at multiple nominal distances in front of the loading axle. Data is recorded at a survey speed of up to 60 mph. The TSD data were used for the road sections where FWD or 3D laser survey van data was unavailable.

### 3.4 GPR

Ground penetrating radar (GPR) is widely used in pavement inspection because it is designed for non-destructive measurement of pavement depth and condition by launching electromagnetic waves into the scanned volume and looking for reflections from the targets. The radar detects the reflected signals transmitted at different frequencies to detect the change in dielectric constant between layers of pavement. In GPR survey, INDOT uses antenna packages which are pulled just over the surface of the road in the direction of travel on both left and right wheel path of the survey

vehicle. The GPR application creates images of the area of interest which are the regions of varying dielectric constant e.g., antenna-to-air, air-to-asphalt, asphalt-to-concrete, concrete-to-base etc. These images are used to determine the pavement depth and types based on the detected layers. The GPR data was used in processing the FWD data for different pavement types. It will also be used in the pavement management tool to calculate the patching depth. We have GPR data for 5.4 miles of SR 243 RF 0-5.4 at a resolution of 1.6 ft.

## 4. GEOSPATIAL DATA FUSION OF PCI PARAMETERS

Vehicle-mounted IRI is an especially popular method of pavement assessment due to its ease of measurement and high resolution over long distances. Even though pavement condition indices (PCI) like IRI and crack density are successful in characterizing pavement rideability, they do not properly account for the effect of pavement structural conditions. Typically, the relation between the surface and structural conditions of the road is probabilistic, yet researchers have not been able to correlate the PCI and structural condition measurements (Gkyrtis et al., 2021; Rada et al., 2012). The structural condition of the pavement is usually measured by the FWD, and structural number index calculated from the FWD center deflection. Comprehensive pavement maintenance requires both surface and structural condition assessments. Thus, an information fusion of the surface and structural condition parameters is desirable to generate a comprehensive pavement condition assessment. Integrating the IRI, CD, and FWD measurement data spatially can allow both local distress detection and overall road structural condition using the high-resolution surface condition parameters and FWD DBPs, respectively.

### 4.1 Geospatial Data Fusion

The high resolution IRI and crack density values were merged with the FWD basing parameters by their geo-index. The geo-index of FWD was matched to the closest geo-index for IRI using the haversine formula. It calculates the great-circle distance between two points on a sphere using their latitude and longitude according to the law of haversine.

The central angle  $\theta$  between any two points on a sphere is:

$$\theta = \frac{d}{r}$$

where:

- $d$  is the distance between the two points along a great circle of the sphere (see spherical distance), and
- $r$  is the radius of Earth (6,371 km).

The *haversine formula* allows the haversine of  $\theta$  (that is,  $\text{hav}(\theta)$ ) to be computed directly from the latitude

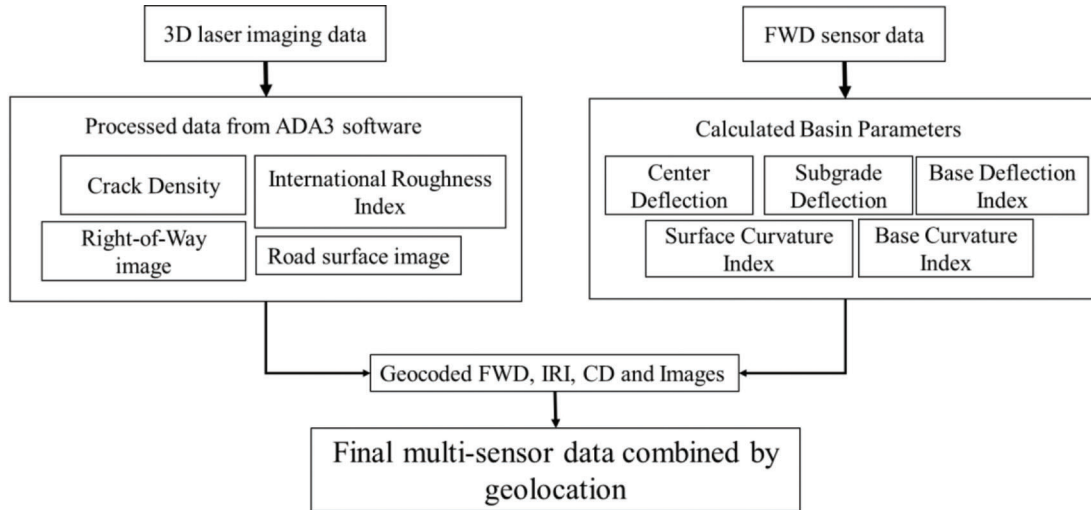


**Figure 4.1** Flow diagram of sensor data fusion.

(represented by  $\phi$ ) and longitude (represented by  $\lambda$ ) of the two points:

$$hav(\theta) = hav(\phi_2 - \phi_1) + \cos(\phi_1) \cos(\phi_2) hav(\lambda_1 - \lambda_2)$$

where:

- $\phi_1, \phi_2$  are the latitude of point 1 and latitude of point 2,
- $\lambda_1, \lambda_2$  are the longitude of point 1 and longitude of point 2.

Finally, the distance  $d$  is

$$d = 2r \arcsin(\sqrt{hav(\theta)})$$

The IRI and FWD with minimum  $d$  value were tagged with the same spatial index. The spatial index was conditioned to have only one nearest value for each 3D laser and FWD data. The GPR data was also merged using the same method. The 2D road surface images and ROW images were mapped to geo-indexed data using unique DMI numbers for each road section. The flow diagram of the data fusion is shown in Figure 4.1.

## 4.2 Evaluation of the Fused Data

### 4.2.1 Comparison of Overall Road Conditions

Interstate highway I-70 was used as a representative full-depth asphalt pavement to determine whether the PCA parameters can be used to assess overall road conditions. Figure 4.2 draws the comparison of FWD deflection parameters across the road classifications. Here, the bottom edge of the rectangle denotes the first quantile (25%) mark, and the upper edge of the rectangle denotes the third quantile (75%) mark in the PCA parameter measurements. The mean of this data is represented by the black triangle and the median by the brown horizontal line. The length of the black vertical lines denotes the range of the data while the minimum and maximum values are shown at the edges of these

lines. The brown point markers represent the possible outliers in the dataset. Since interstate highway is typically designed with stronger pavement structures to support heavier traffic volume, overall FWD deflection parameters are lower than on U.S. highways and state roads. This means that the FWD deflection parameters can be used as structural indicators to represent overall road conditions.

### 4.2.2 Evaluation to Detect Localized Faults.

Identifying localized distresses is the major expectation from the PCA parameters in providing accurate geo-location of road sections with maintenance requirements. Spatially integrated IRI and FWD deflection parameters were compared with the crack density, road surface and ROW images to determine whether these parameters can successfully capture the localized distresses of in-service full-depth asphalt pavements. Stem plots were drawn to compare the values of IRI, CD and FWD basin parameters and select the DMIs with PCA values in medium and high ranges. These ranges were initially set using the current maintenance threshold values used by INDOT.

The highest value of L-IRI, 8.1 m/km was observed at the left wheel path DMI 2922, on I-70-WB-PL as shown in the plot in Figure 4.3a. This value is also greater than the interstate IRI threshold value. The road surface and ROW image of the same DMI 2922 captured from the WayLink software shows localized patching for pothole on the left edge of the road, marked with a red arrow in Figure 4.3b. Similarly, left and right IRI values, R-IRI 7.7 m/km and L-IRI 5.4 m/km, were greater than the IRI threshold value at DMI 330. The high L-IRI value is shown in the stem plot in Figure 4.3c. A strip patching was captured at DMI number 330 on the same section of I-70 as shown in Figure 4.3d. As shown in Figure 4.4a and Figure 4.4b, the authors were also able to locate DMI with a high



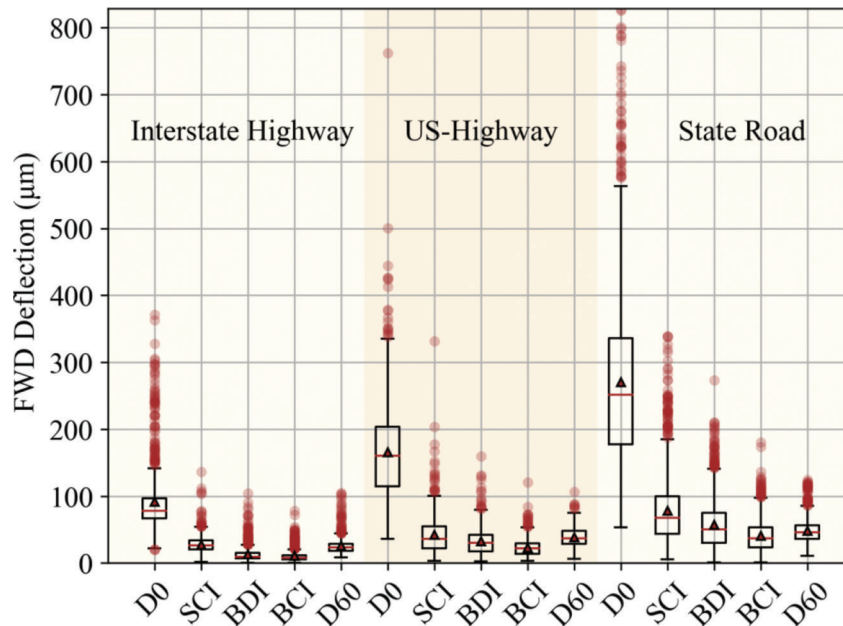


**Figure 4.2** Comparison of FWD deflection parameters from all road classifications.

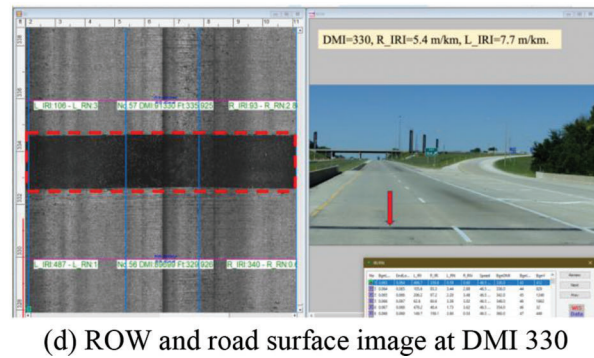
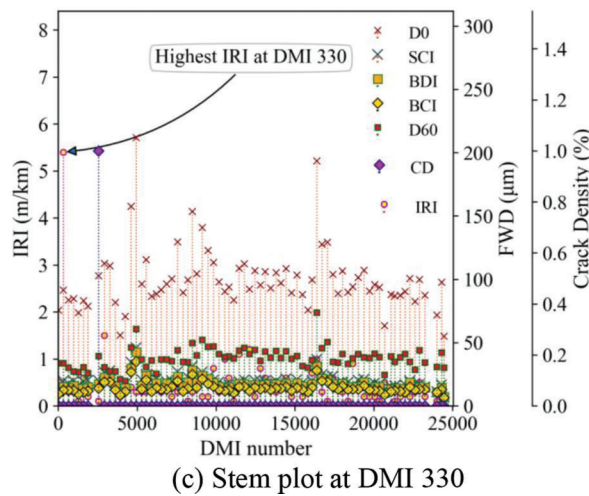
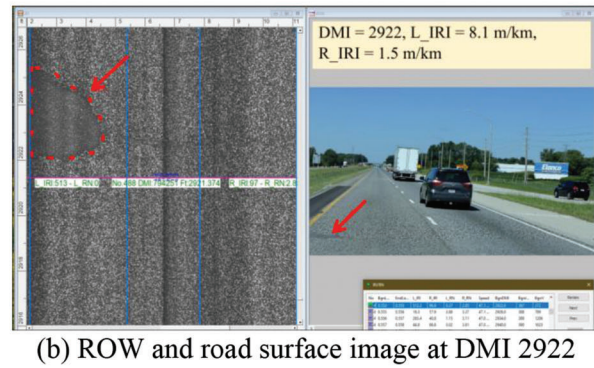
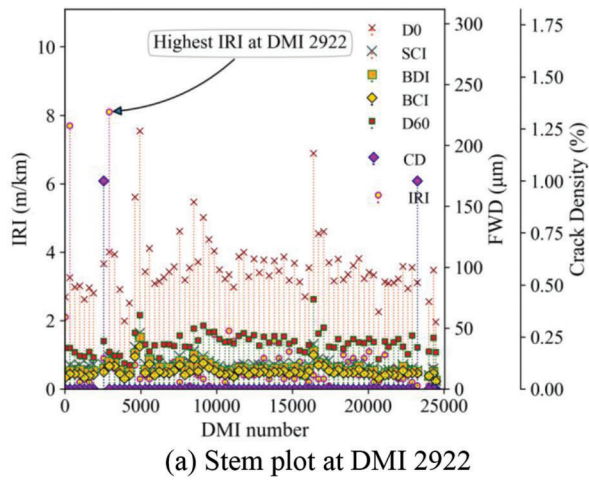


**Figure 4.3** IRI data from WayLink ADA3.

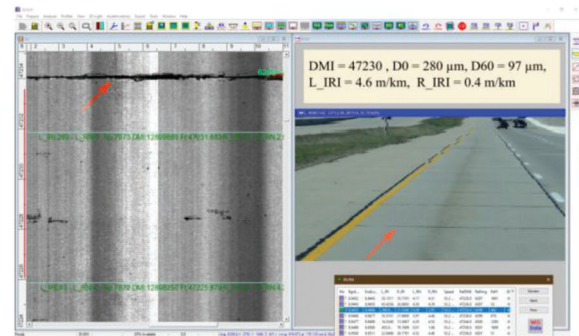
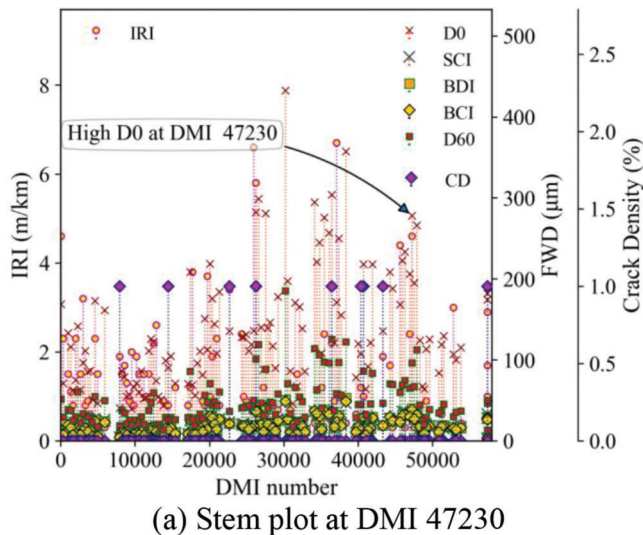


**Figure 4.4** DMI with high IRI, FWD deflections, and CD identified (a) using stem plot, and (b) the ROW and road surface image for the identified DMI on I-70 from WayLink.

center deflection on the I-70 westbound road. A center deflection value of 280 microns was captured at this DMI 47230, which is higher than the calculated threshold value, and cracks are easily visible on the road surface and ROW image in the WayLink software. The authors have extensively checked the ability of the 1.8-m resolution data to detect localized distresses by selecting assessment index values exceeding their upper threshold values from scatter plots and comparing them to their corresponding ROW image and road surface image. These findings confirm that the selected PCA parameters accurately detected localized distresses and other features on roads such as crack sealing, small patching, uphill, downhill, turns, railroad crossings, etc., from road condition parameter data alone. The stem plots and the ADA3 software was used extensively to check and validate the PCA values on different road sections.

## 5. THRESHOLD CALCULATION AND PATCHING SUGGESTION ALGORITHM

### 5.1 Determination of FWD Parameters Thresholds

Thresholds of FWD parameters were preliminarily determined based on the concept of design reliability, which is the probability of good pavement sections over the design period. According to the *Mechanistic-Empirical Pavement Design Guide*, the reliability concept is recommended for determining performance threshold values to achieve a balance between maintenance costs and overall pavement structural health (AASHTO, 2020). In this study, a reliability analysis was conducted using the INDOT FWD database to determine preliminary thresholds of FWD parameters. Since threshold values determined by the reliability concept are dependent on the current condition of the pavements, further verification was needed to determine whether the reliability-based approach can

provide reasonable thresholds for the structural assessment of the pavements. Therefore, the prevalent structural condition index, structural number ratio (SNR), was used to verify the preliminary threshold values. This section describes the steps in the process of calculating the FWD parameter threshold values in detail, which include (1) determining the preliminary thresholds using the reliability, and (2) verifying the preliminary thresholds using the SNR.

### 5.2 Determination of Preliminary FWD Thresholds Using Reliability

Two threshold values were selected to define three levels of pavement structural condition as good, fair, and poor. For each road classification, two reliability levels were selected at 5% intervals, based on the recommended level of reliability in the AASHTO 1993 design guide (AASHTO, 1993). Interstate highways used 90% and 95% for lower and upper limits, US-Highways used 85% to 90% of reliability levels, and state roads used 80% to 85% respectively. Since a road with heavier traffic typically requires a higher level of reliability, the highest reliability levels were selected for the interstate highway and the lowest for state road. The higher reliability value was used as the threshold between poor and fair pavement conditions, while the lower reliability value was used as the threshold between fair and good pavement conditions. It should be noted that these reliability levels have been used and verified by previous researchers to determine thresholds of structural indicators (Bryce et al., 2019; Flora et al., 2010). Furthermore, similar percentage levels were observed and used by previous researchers to distinguish good and acceptable roads based on the IRI and ride quality index in its *state highway reliability report* by INDOT very recently (FHWA, 2022).

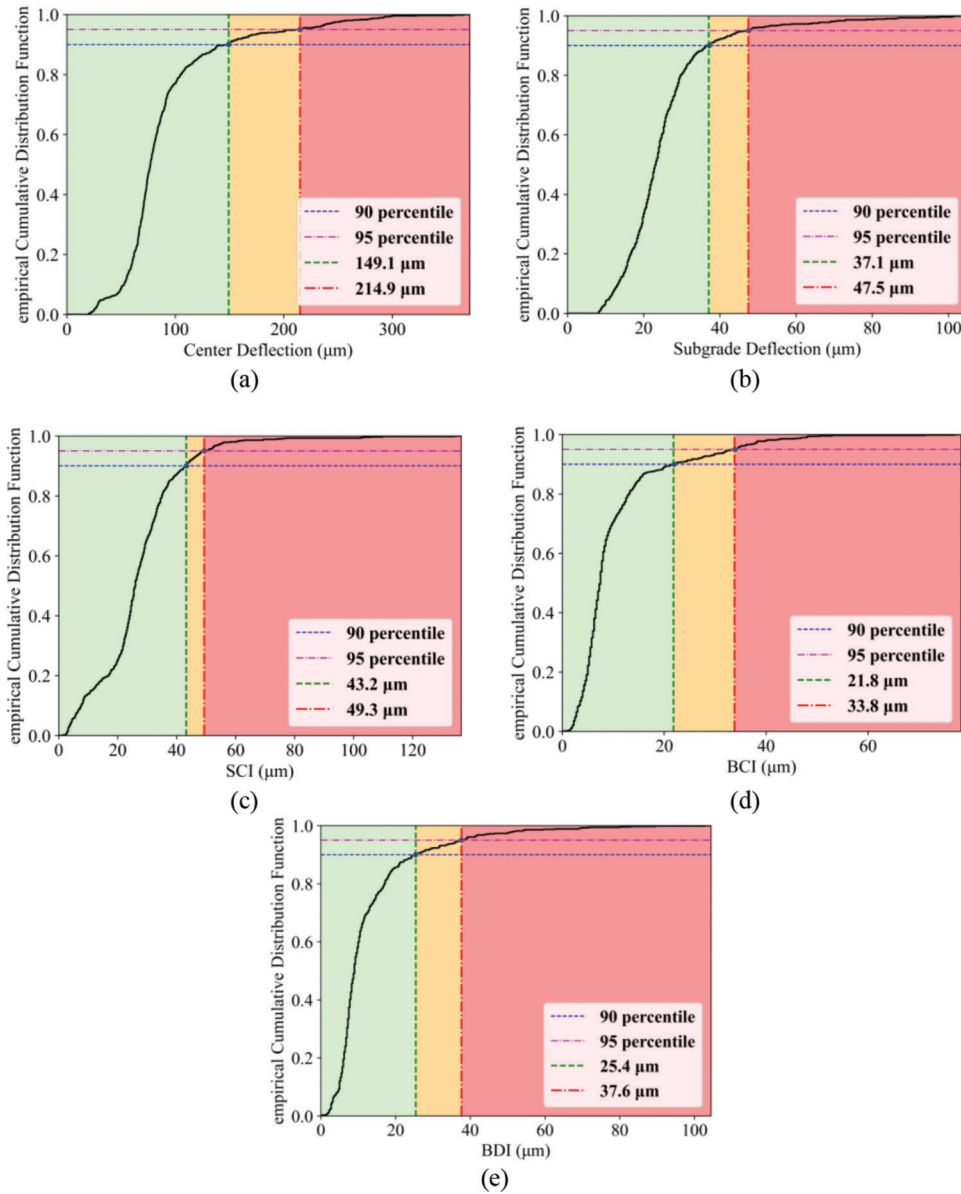


**Figure 5.1** ECDF plot for FWD deflection parameters on interstate full-depth asphalt pavement: (a) center deflection (D0), (b) subgrade deflection (D60), (c) SCI, (d) BCI, and (e) BDI.

The FWD data collected from the INDOT pavement management system (PMS) database was used for reliability analysis. The total number of FWD data points was 1,579, 605, and 717 for state roads, US-highways, and interstate highways, respectively. The empirical cumulative distribution function (ECDF) was used to conduct the reliability analysis for determining preliminary threshold values of FWD parameters; it is an estimate of the cumulative distribution of each data point in the measured samples. To illustrate the role of ECDF, we have plotted the ECDF values against the FWD deflections, measured on interstate highway as shown in Figure 5.1 ECDF plot for FWD deflection parameters on interstate full-depth asphalt pavement: (a) center deflection (D0), (b) subgrade deflection (D60), (c) SCI, (d) BCI, and (e) BDI.

For example, the D0 values 214.9 and 149.1 microns correspond to the reliability levels 95% and 90%, meaning 95% of the D0 measurements are below 214.9 microns and 90% of the D0 measurements are below 149.1 microns among the total D0 measured on interstate highways in the scope of this study. Thus, we classify the interstate highway locations with D0 greater than 214.9 microns as poor road conditions. The same approach was applied to other FWD parameters as shown in Figure 5.1.

The reliability results of FWD deflection parameters for the three distinct types of roads are summarized in Table 5.1. The values of the FWD parameter, corresponding to four reliability levels (80%, 85%, 90%, and 95%) are also presented in Table 5.1. Furthermore, it was found that the state road exhibited the greatest



TABLE 5.1  
Reliability Results of FWD Deflection Parameters

Road Type	Percentage (%)	D0 (microns)	D60 (microns)	SCI (microns)	BCI (microns)	BDI (microns)
State Road	<b>80</b>	<b>359.9</b>	<b>59.4</b>	<b>111.0</b>	<b>57.2</b>	<b>81.5</b>
	<b>85</b>	<b>388.6</b>	<b>62.2</b>	<b>123.2</b>	<b>62.2</b>	<b>89.2</b>
	90	423.7	67.3	138.7	68.1	102.9
	95	494.3	77.5	171.2	82.6	125.0
U.S. Highway	80	212.9	50.5	58.9	30.5	45.5
	<b>85</b>	<b>227.6</b>	<b>53.1</b>	<b>66.0</b>	<b>34.3</b>	<b>50.0</b>
	<b>90</b>	<b>259.8</b>	<b>56.6</b>	<b>76.7</b>	<b>39.1</b>	<b>55.9</b>
	95	295.4	63.0	94.0	46.2	68.6
Interstate Highway	80	106.4	30.2	35.6	13.2	17.3
	85	121.4	33.0	38.1	15.5	19.6
	<b>90</b>	<b>149.1</b>	<b>37.1</b>	<b>43.2</b>	<b>21.8</b>	<b>25.4</b>
	<b>95</b>	<b>214.9</b>	<b>47.5</b>	<b>49.3</b>	<b>33.8</b>	<b>37.6</b>

Note: The percentile threshold range of FWD deflections for each road type is in boldface.

values of FWD deflection parameters, while the interstate highway showed the lowest values at the same reliability level. This is a reasonable trend because a conservative threshold value should be applied to the road with heavier and faster traffic (i.e., interstate highway) to maintain better conditions in comparison with state roads or U.S. highways which have lower traffic volume. Similarly, the preliminary threshold values for all FWD deflection parameters are highlighted in Table 5.1.

### 5.3 Verification of FWD Thresholds Using the Structural Number Ratio (SNR)

SNR is derived from the concept of a pavement structural number developed by the American Association of State Highway Officials (AASHTO), and it has been widely used in PMS to evaluate the structural capacity of in-service asphalt pavements (Kim et al., 2013; Zhang et al., 2003). As expressed in Equation 5.1, the SNR is the ratio of the effective structural number ( $SN_{eff}$ ) and the required structural number ( $SN_{req}$ ) (Abd El-Raof et al., 2018; Rohde, 1994). The  $SN_{eff}$  indicates the structural number of existing asphalt pavements, and the  $N_{req}$  is the minimum structural number to ensure a desirable structural performance over the design period. Theoretically, the  $SN_{eff}$  should be greater than the  $SN_{req}$  to achieve adequate structural performance, and the minimum SNR requirement is one.

$$SNR = \frac{SN_{eff}}{SN_{req}} \quad (\text{Eq. 5.1})$$

The AASHTO 1993 pavement design guide dictates the methods to determine the  $SN_{eff}$  and  $SN_{req}$  using the FWD deflection data. The  $SN_{req}$  can be determined by solving Equation 5.2, and input parameters are a subgrade resilient modulus ( $M_R$ ), equivalent single axle load (ESAL), reduction in serviceability ( $\Delta PSI$ ),

standard deviation ( $S_0$ ), and standard normal deviate ( $Z_R$ ). In this study, the FWD deflection measured at 1,524 mm (60 in.) away from the loading center was used to calculate the  $M_R$ . It should be noted that upper layers (i.e., asphalt base layer) may affect deflections measured from nearer sensors (D48 or D36) because strong structures of full-depth asphalt pavements result in a wider stress zone. Thus, the D60 was selected to accurately estimate the  $M_R$  of full-depth asphalt pavements. The same ESAL was assumed for each road classification, based on the ESAL category dictated in the INDOT specification. The state road used one million ESALs, while U.S. highway and interstate highway used four million and 10 million ESALs, respectively. In addition, 1.701 of  $\Delta PSI$  and 0.35 of  $S_0$ , which are recommended in the INDOT specification, were used. The  $Z_R$  was determined based on the reliability levels following the AASHTO 1993 design guide: -1.037 for an 85% reliability level, -1.282 for a 90% reliability level, and -1.645 for a 95% reliability level. It should be noted that the same reliability levels used for the reliability analysis were applied to the  $SN_{req}$  calculation (i.e., state road: 85%, US highway: 90%, and interstate highway: 95%).

$$\log ESAL = Z_R \times S_0 + 9.36 \times \log(SN_{req} + 1) - 0.2 + \frac{\log\left(\frac{\Delta PSI}{4.2 - 1.5}\right)}{0.4 + \frac{1.094}{(SN_{req} + 1)^{3.19}}} + 2.32 \times \log M_R - 8.07 \quad (\text{Eq. 5.2})$$

$$M_R = \frac{0.24 \times P}{d_r \times r}$$

where ESAL is the equivalent single axle load,  $\Delta PSI$  is a reduction in serviceability,  $S_0$  is a standard deviation,  $Z_R$  is a standard normal deviate,  $M_R$  is a subgrade resilient modulus (ksi),  $P$  is the FWD load (lbs.),  $r$  is a distance from the center of load (in.), and  $d_r$  is a deflection at a distance  $r$  from the center of the load (in.).

According to the AASHTO 1993 design guide, the  $SN_{eff}$  can be determined using the total pavement thickness and the effective modulus of existing pavements obtained from the FWD data. However, the AASHTO 1993 method requires a trial-and-error procedure to obtain the pavement effective modulus, which is a key parameter for  $SN_{eff}$  calculation and is impractical to be incorporated into the network-level PMS. Furthermore, the AASHTO 1993 method is significantly dependent on the pavement thickness, resulting in overestimated  $SN_{eff}$ . Thus, previous researchers have developed alternative models to estimate the  $SN_{eff}$  using the FWD deflection data, without a trial-and-error procedure (Crook et al., 2012; Kavussi et al., 2017; Rohde, 1994). Recently, a new  $SN_{eff}$  prediction model was developed and verified with field data in a concurrent study conducted by INDOT. As expressed in Equation 5.3, the new model only requires a total pavement thickness and the FWD deflection basin parameter, the area under pavement profile (AUPP), to make accurate predictions of  $SN_{eff}$ . Therefore, this study adopts this new model to calculate the  $SN_{eff}$ .

$$SN_{eff} = 2.272 \times H_p^{0.4217} \times AUPP^{-0.4678} \quad (\text{Eq. 5.3})$$

where,  $H_p$  is the pavement thickness above subgrade (in.), and AUPP is the area under pavement profile (mils).

The maximum FWD deflection D0 was selected as a representative FWD parameter to compare with the preliminary threshold values calculated using reliability analysis since both D0 and SNR represent the overall structural conditions of existing pavements. Other FWD parameters are typically used to estimate the structural conditions of specific layers (i.e., surface layer, base layer, and subgrade layer), indicating that a different more specific structural index may be needed to compare with the other FWD parameters. However, there are currently no available structural indices for individual layers. Therefore, the reliability-based approach was extended to the other FWD parameters to determine the final threshold values if the D0 thresholds match with thresholds calculated from SNR.

Figure 5.2 shows that the SNR decreased as D0 increased with an exponential relationship, for all road classifications, including state roads, U.S. highways, and interstate highways. Based on the relationship, the D0 values, corresponding to the SNR limit were identified to establish the D0 threshold range for each road classification. As shown in Figure 5.2, the D0 threshold of state roads ranged from 125 to 400 microns, and the D0 threshold range was 120 to 254 microns for U.S. highways and 100 to 203 microns for interstate highways. Overall, the threshold of state roads was greater than the threshold of interstate highways. This trend is consistent with the standard pattern and was also observed in reliability-based threshold values. Interestingly, for all road classifications, the upper limit of the threshold range was almost identical to highlighted D0 threshold value from the

reliability analysis in Table 5.1. For example, the upper limit of the reliability-based threshold of D0 for state road (388.6 microns) was slightly smaller than the upper limit of the D0 threshold identified based on the SNR analysis (400 microns). Therefore, the threshold calculated from the reliability analysis of current road conditions was verified with a similar threshold range obtained from SNR calculation. Hence, it was used to distinguish good, fair, and poor structural conditions of full-depth asphalt pavements, and the final threshold values of FWD deflection parameters are presented in Table 5.2.

## 5.4 Determination of Functional Parameters Thresholds

Thresholds of IRI and CD were determined using the reliability percentile values verified by the threshold comparison results of FWD deflection parameters. Figure 5.3 shows ECDF plots of IRI and CD for interstate highway. The 95% and 90% reliability levels were used for rating the pavements into good, fair, and poor conditions. Accordingly, the higher IRI threshold value was 2.07 m/km, and the lower IRI threshold value was 1.73 m/km. Similarly, the higher threshold of CD was 1.3%, while the lower threshold value for CD was 1.6%. It is important to note that thresholds of IRI and CD were determined only for full-depth asphalt pavement and interstate highways, as IRI and CD data collection is ongoing for state roads and U.S. highways. Thus, in this study, interstate highway was used to verify the concept and algorithm for patching suggestions.

## 5.5 Evaluation of Geo-Indexed Data Using Calculated Threshold Values

The overall conditions of the driving lane (DL) and passing lane (PL) for both eastbound (EB) and westbound (WB) roads were analyzed using central tendency plots shown in Figure 5.4, by comparing their mean and median values. Here, the red dots are points in the high severity range which represent road locations in poor condition, the yellow dots are in the medium severity range, i.e., locations with fair road conditions, and the green dots are in the low severity range, i.e., locations with good road conditions. Thus, the red and yellow point markers represent the PCA parameter measurements at locations which were selected as candidates for maintenance by the patching suggestion algorithm. The black quadrilaterals and black horizontal lines are the mean and median of the PCA parameters on the plotted road sections. Overall, this plot shows that both right-wheel IRI and left-wheel IRI values of the driving lane are greater than those in the passing lane for both EB and WB, illustrated by their comparatively higher mean and median values. Usually, a driving lane has more wear than a passing lane, due to higher traffic volume on the driving lane. This indicates that the functional parameters can correctly compare the overall functional condition of

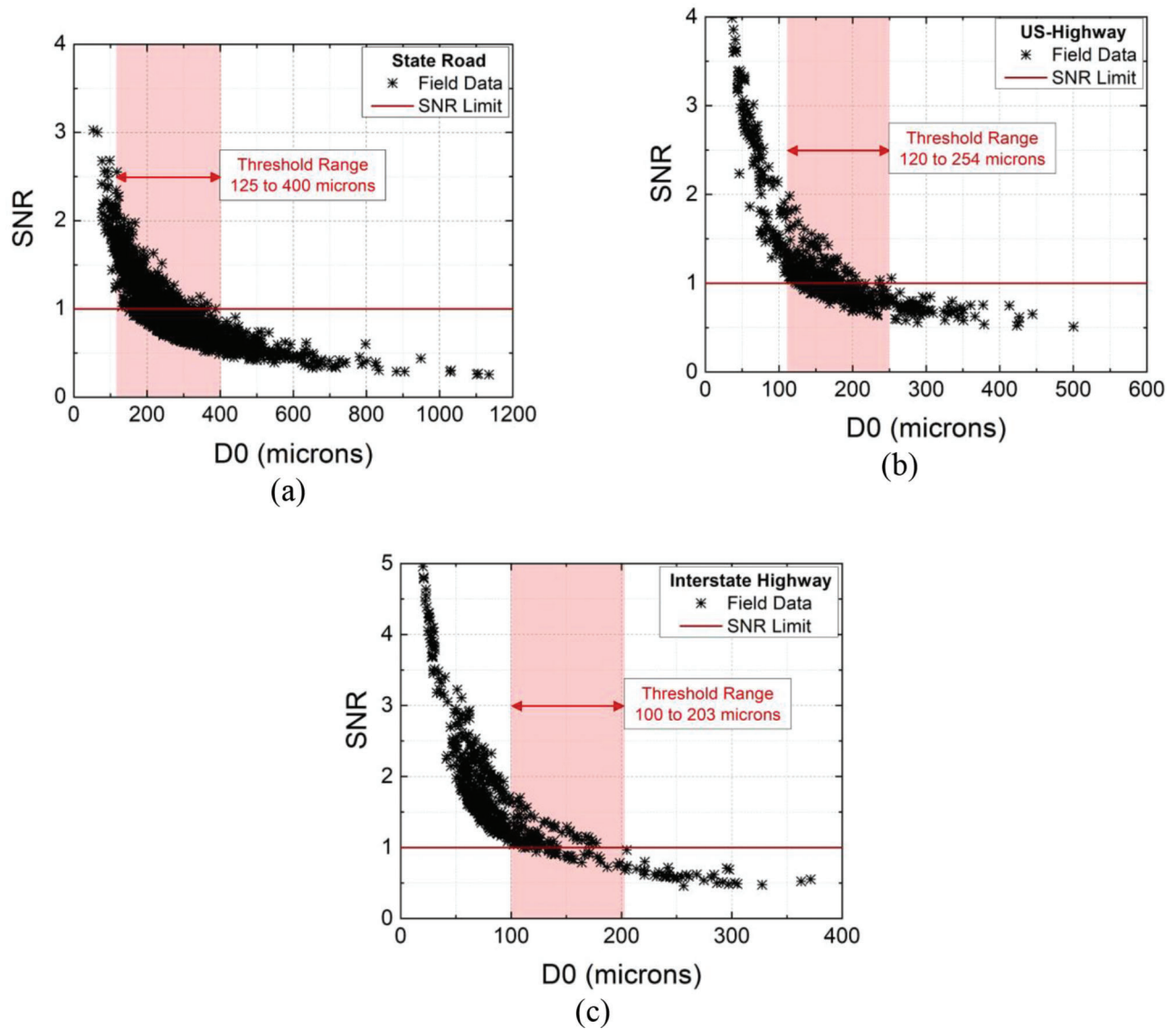


**Figure 5.2** Comparison between SNR and D0: (a) state road, (b) U.S. highway, and (c) interstate highway.

lanes using the central tendency parameters and detect road locations which require attention.

As shown in Figure 5.4a and Figure 5.4b, a similar trend was observed from D0 and D60 on the same road section on I-70. Both the D0 and D60 values of the driving lane were greater than the passing lane based on the central tendency parameters. As expected, the driving lane results exhibited higher variations in both D0 and D60 compared to passing lane results, represented by higher mean and median values and significantly high deflection measurements. Higher traffic density on driving lanes exacerbates the pavement stress causing greater deflection values and increased variation in the distribution of D0 and D60.

## 5.6 Patching Suggestion Algorithm

Pavement surface patching and full-depth patching were used as the patching depth suggestions in the

surface condition evaluation. Surface patching and full-depth patching are defined according to the AASHTO pavement maintenance protocol. Patching required and patching warning was similarly used as patching priority suggestion. Patching required has higher priority in maintenance than patching warning. Figure 5.5 illustrates the classification of the state of the three pavement layers into five conditions for patching. The underlying rectangular shapes represent the surface, base/intermediate and sub-base/subgrade layers of a full-depth asphalt pavement. The red, orange, and green colored layers represent the current state of the layers. Green represents the good state of layers, i.e., values lower than the lower thresholds of PCA, orange represents the fair state, and red represents the poor state of pavement layers, i.e., PCA values greater than the upper thresholds calculated earlier.

TABLE 5.2  
Final Threshold Values of FWD Deflection Parameters

Road Type	FWD Parameter	Good	Fair	Poor
State Road	D0 (microns)	$D0 < 359.9$	$359.9 < D0 < 388.6$	$388.6 < D0$
	D60 (microns)	$D60 < 59.4$	$59.4 < D60 < 62.2$	$62.2 < D60$
	SCI (microns)	$SCI < 111.0$	$111.0 < SCI < 123.2$	$123.2 < SCI$
	BCI (microns)	$BCI < 57.2$	$57.2 < BCI < 62.2$	$62.2 < BCI$
	BDI (microns)	$BDI < 81.5$	$81.5 < BDI < 89.2$	$89.2 < BDI$
U.S. Highway	D0 (microns)	$D0 < 227.6$	$227.6 < D0 < 259.8$	$259.8 < D0$
	D60 (microns)	$D60 < 53.1$	$53.1 < D60 < 56.6$	$56.6 < D60$
	SCI (microns)	$SCI < 66.0$	$66.0 < SCI < 76.7$	$76.7 < SCI$
	BCI (microns)	$BCI < 34.3$	$34.3 < BCI < 39.1$	$39.1 < BCI$
	BDI (microns)	$BDI < 50.0$	$50.0 < BDI < 55.9$	$55.9 < BDI$
Interstate Highway	D0 (microns)	$D0 < 149.1$	$149.1 < D0 < 214.9$	$214.9 < D0$
	D60 (microns)	$D60 < 37.1$	$37.1 < D60 < 47.5$	$47.5 < D60$
	SCI (microns)	$SCI < 43.2$	$43.2 < SCI < 49.3$	$49.3 < SCI$
	BCI (microns)	$BCI < 21.8$	$21.8 < BCI < 33.8$	$33.8 < BCI$
	BDI (microns)	$BDI < 25.4$	$25.4 < BDI < 37.6$	$37.6 < BDI$

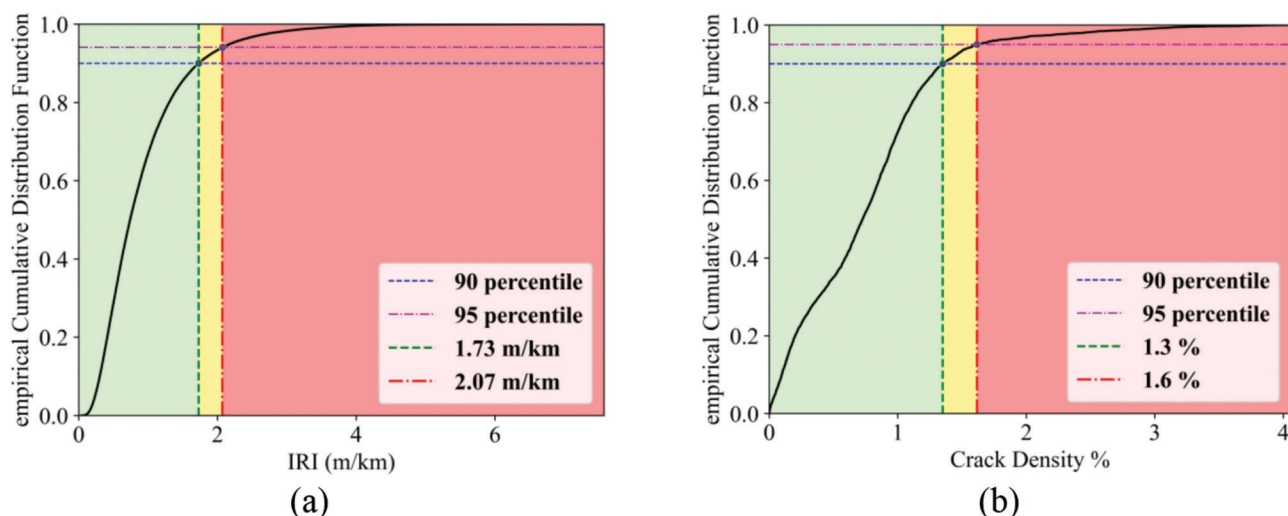


Figure 5.3 ECDF plot for functional parameters of interstate highway: (a) IRI and (b) CD.

*Condition 1* shows the poor condition of the subbase/subgrade layer with a combination of the poor state of the intermediate/base layer. Pavement in this state requires a full-depth patch irrespective of the condition of the surface layer. Similarly, when the intermediate/base layer is in a poor state and the sub-base/subgrade layer is in a fair state, *Condition 2* would be applicable and a warning for full-depth patching would be suggested by the algorithm. Furthermore, the patching suggestion requirement and warning for surface patching are based on two combinations of pavement layer states as shown in *Condition 3* and *4*. *Condition 3* requires surface layer patching determined by the poor

condition of the surface layer with fair state of the base/intermediate layer and good condition of the sub-base/subgrade layer. *Condition 4* indicates warning surface layer patching determined by the fair state of the surface layer and good conditions of base/intermediate and sub-base/subgrade layers. Lastly, *Condition 5* indicates good road conditions where no further action is needed. This conditional patching suggestion algorithm is reinforced by adding pavement type/road classification threshold values.

The threshold-based patching suggestion for interstate highway full-depth asphalt pavement is aggregated in Table 5.3.



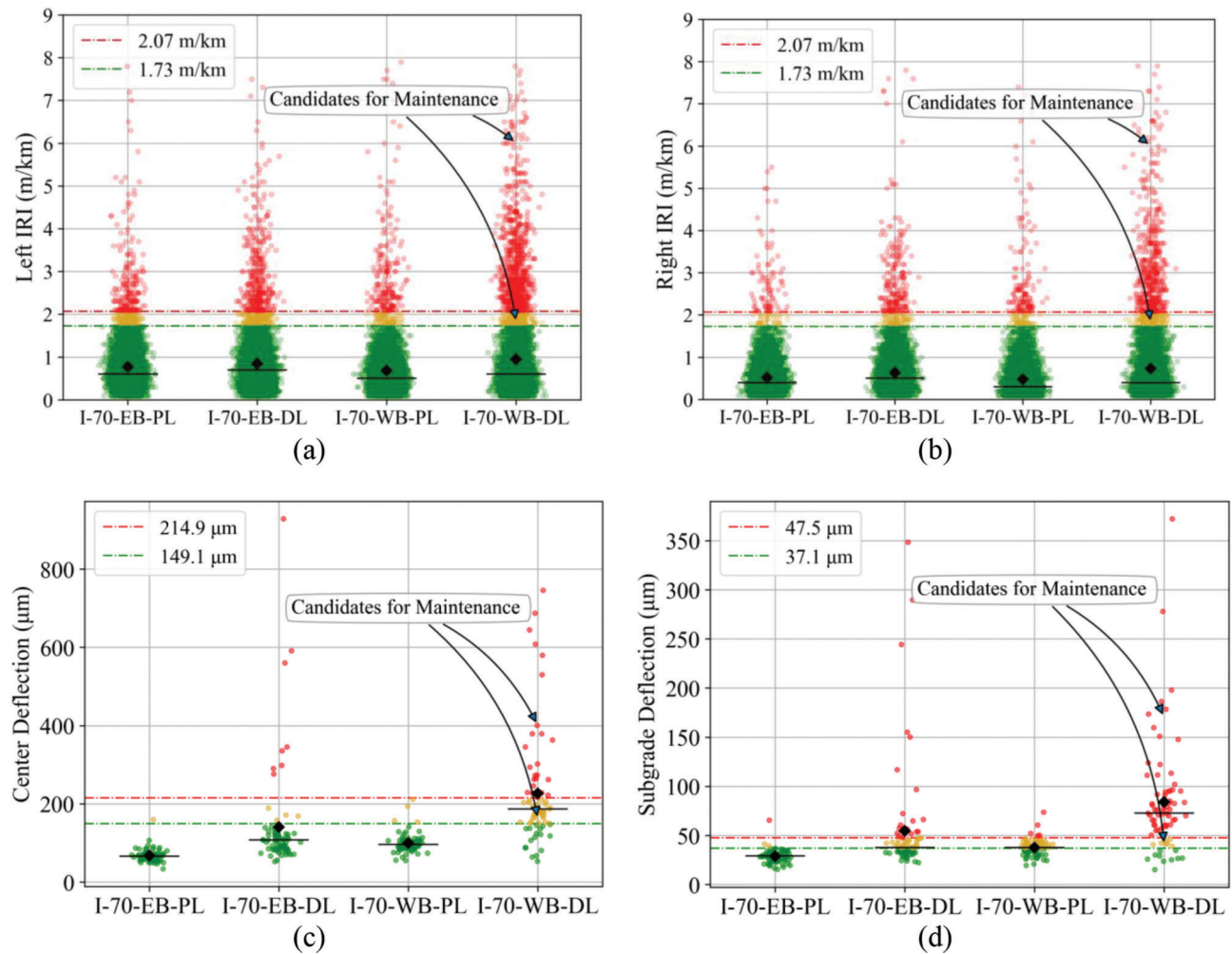


**Figure 5.4** Comparison of IRI and FWD on I-70: (a) left IRI, (b) right IRI, (c) center deflection D0, and (d) subgrade deflection D60. The Y-axis ranges of (c) and (d) are different to conserve the necessary information in both figures.

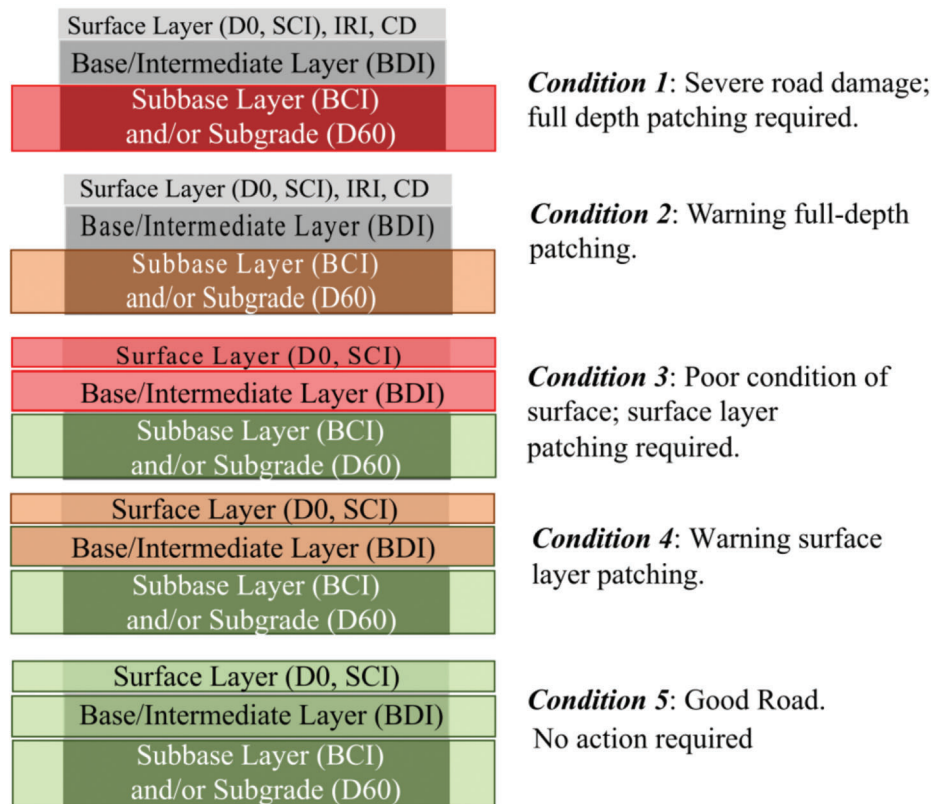


**Figure 5.5** Patching conditions labeled according to the measurement range of FWD deflections.

**TABLE 5.3**  
**Threshold-Based Patching Suggestion Algorithm for Interstate Full-Depth Asphalt Pavement**

IRI (m/km)	CD (%)	D0 (μm)	SCI (μm)	BDI (μm)	D60 (μm)	BCI (μm)	Patching Suggestions
–	–	–	–	–	>47.5	>33.8	Severe road damage; full-depth patching requirement
–	–	–	–	–	>37.1 & ≤47.5	>21.8 & ≥33.8	Full-depth patching warning
>2.07	>13.2	>214.9	>49.3	>37.6	≤37.1	≤21.8	Poor condition of surface layer; surface patching required
>1.73 & ≤2.07	>12.5 & ≤13.2	>149.1 & ≤214.9	>43.2 & ≤49.3	>25.4 & ≤37.6	≤37.1	≤21.8	Surface patching warning
≤1.73	≤12.5	≤149.1	≤43.2	≤25.4	≤37.1	≤21.8	No action required

Note: The patching suggestions are highlighted in red text to represent a high priority action requirement. Blue text represents a medium priority warning. Green text represents good condition roads where no action is required.

## 6. PMT WEB-APPLICATION

The PMT web-application encapsulates managing a static database for the PCA parameter raw data, as shown in Figure 6.1. These include 2D road surface images and ROW images for all road sections along with the text datafiles for PCA parameters. The static database would be used to fetch image data. The static database was hosted using simple python HTTP server on a Purdue machine with 5Tb storage space.

### 6.1 Current database

The PMT static database contains IRI, CD, FWD, GPR, TSD, road surface images, right-of-way ROW images. There are 155,267 center mile (~621.1 lane miles) of processed IRI, CD, and Image data in the PMT database. This includes 1.01 GB (PMT patch tables) + 1.14 TB (images) and 3.09 TB raw 3D laser sensor data. FWD data for 213.04 miles measured at least every 300 ft are text files of total size 2 MB. GPR depth information for 5.4 miles at every 1.6 ft. is 14.2 MB and TSD data for 192.5 miles measured every 52.4 ft. = 24 MB. As per our current calculations the size of data per lane mile when all the PCA parameters are present is 1.831 GB. It includes CSV data (0.82 MB + 0.82 MB (GPR) = 1.64 MB) and Image data (282.4 MB (ROW) + 775 MB + 775 MB = 1.83 GB). We projected the size of database using this information for the total number of miles of road in Indiana, which are about 29,800 miles (roughly 1,000 centerline miles), to 54 TB. The processed FWD data is first merged with the processed IRI data from ADA3 software. Then the thresholds are calculated and added to the patching suggestion conditional inequality. After this the image

DMI location hyperlinks from the python server are mapped to their DMI numbers in the final patching suggestion data table. All these steps are done using python and then stored in the database as patching tables. The PMT web application fetches the data from the python HTTP server using the chrome browser settings.

### 6.2 Geospatial Data Processing

The roads in the datasets were divided into sections of different sizes. Some sections were only a couple of miles long, while others were around 20 miles or larger. The reference points on the roads are marked the same for each lane, which means that between fixed reference points there could be multiple lanes. So, a 12-lane road like I-465 RP 09.07-16.45 has 266,640 geographical points in the 25.25-mile section. Plotting such a large number of points on a web browser increases the loading time of the application due to the sheer number of points. This slow rendering issue was resolved by creating line strings of points which represented aggregated data of good condition roads. On most roads, 90% to 95% of points/locations were found to be in good condition and were grouped into a single line geometry with values equal to the central tendency of the grouped points. This allowed faster rendering of large number of points even for I-465.

### 6.3 Patching Management Tool

A web-based application can be hosted on an internet browser and hence is easily available to view with credentials. The open-source structure of the application also makes it free to use for individual

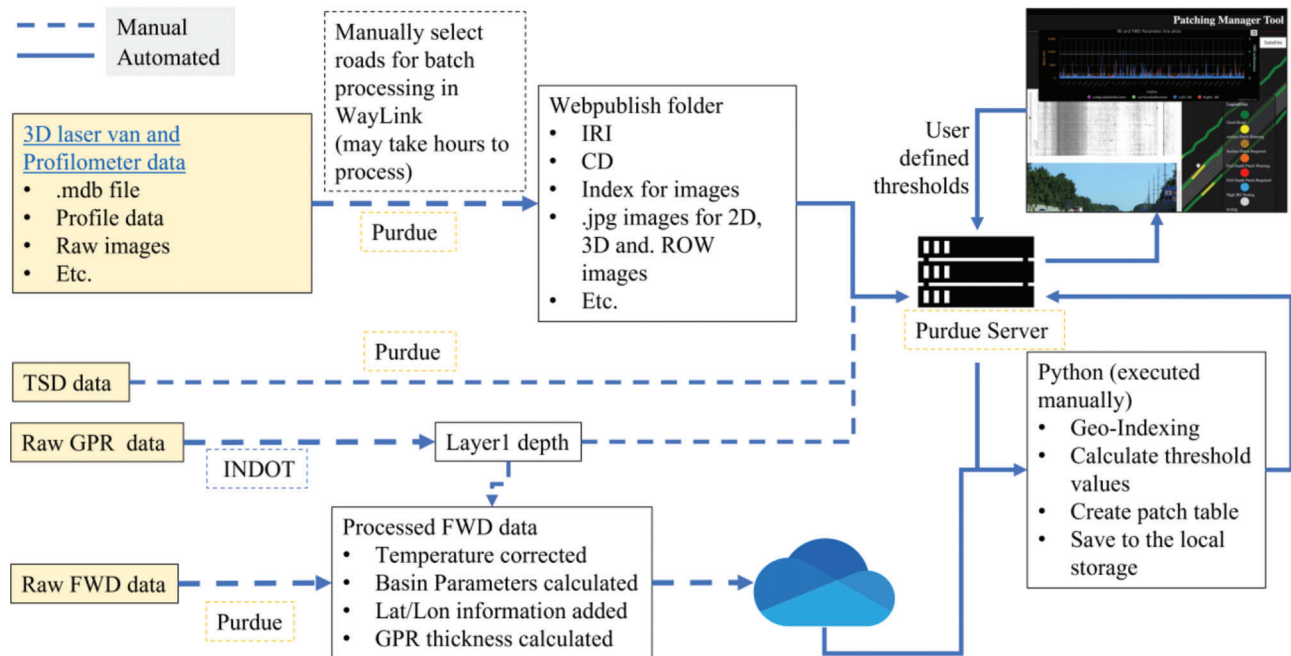
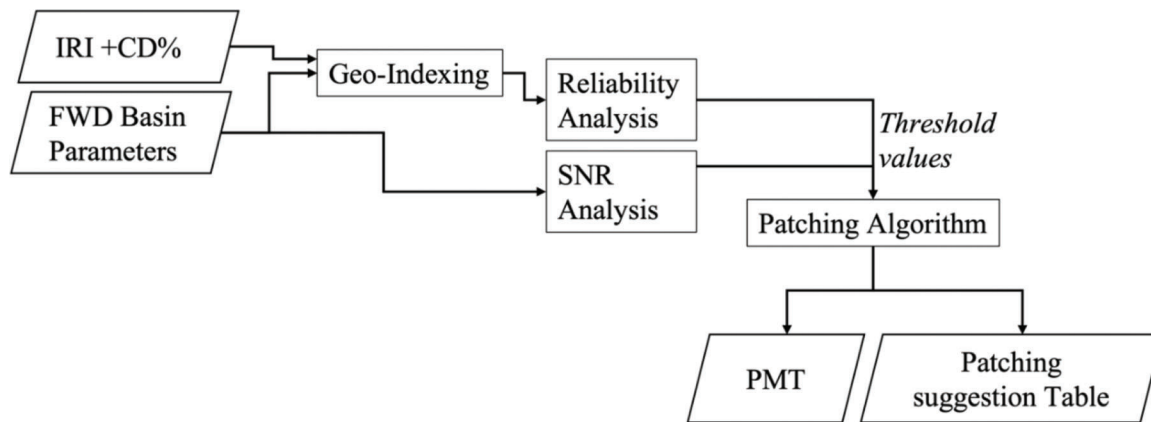


Figure 6.1 The data flow structure in the PMT web application.



**Figure 6.2** The flow diagram of processing the raw data for the patching manager tool (PMT).

analysts/engineers. In the PMT application, the threshold-based patching algorithm is currently implemented using the spatially indexed and integrated PCA parameters to create patching suggestions for roads of interest. Using the application, patching suggestions can be downloaded which include location co-ordinates, PCA parameter measurement values, suggested parameter severity ratings, patching information (i.e., area, depth, quantity, and priority suggestion), and pavement information (i.e., road name, pavement type, reference point (RP) and lane). Figure 6.2 illustrates a block diagram which shows the flow diagram of processing the raw data until publishing it on PMT.

The developed web application has three major functionalities. Once a road of interest is selected, it creates a table with patching location and quantity suggestions, which is presented as color-coded visualization on the geographical map of Indiana. Colored markers are used to represent pavement sections of 1.8 m in length and 3.6 m in width, as shown in Figure 6.3. These markers are identified by unique DMI numbers and geographical coordinates. The marker color represents patching depth and priority. For example, the red markers represent high priority full-depth patching requirement, the orange markers mean a warning for full depth patch, the yellow markers warn that a surface patch may be needed, and the green marker represents good road locations.

The patching manager tool also supports distress data analysis features, which include histogram analysis and scatter plot analysis of pavement rating parameters. These analysis tools are necessary to analyze the values at the location nearest to the distress to understand its probable causes. The causes of distress are crucial factors in determining the maintenance suggestions. The potential of the web application is placed in its data-driven ability to allow users to compare road conditions at distressed locations which may be miles apart.

The patching suggestions provided by PMT were compared with the Google Street View feature in PMT for further validation using different road sections. One

such example on road I-64 used for this verification is discussed here. A particular DMI 24204 on I-64 EB DL is shown in Figure 6.4, which was selected from the patching suggestion visualization, and the street view at this DMI was explored. PMT suggests a warning for surface patching at DMI 24204 shown with a yellow marker because the IRI at this location was greater than its lower threshold value. Therefore, it was confirmed that PMT accurately suggests patching suggestions at genuinely distressed locations, also captured in the Google Street View map.

## 6.4 PMT Web-Application Design

The pavement patching management tool was envisioned as an open-source light weight application to be used on web browsers to use the reliability based patching suggestions. The PMT was made with the following characteristics.

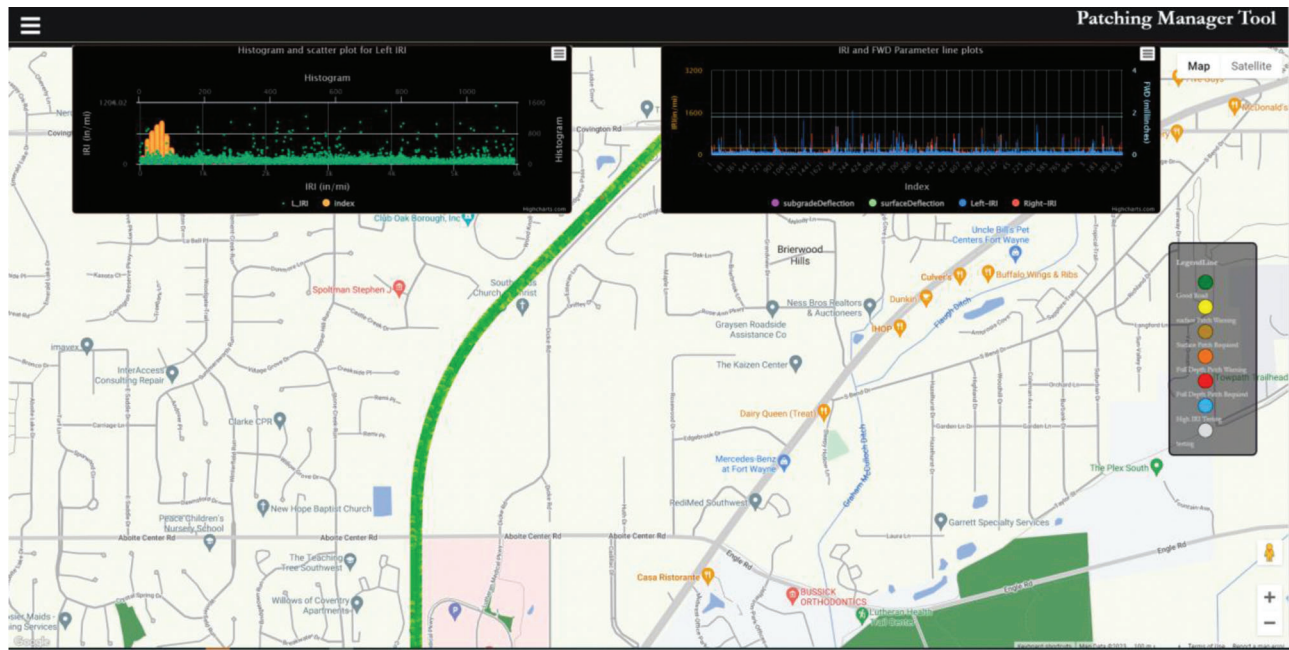
### 6.4.1 Flexibility in Design and Use

Writing a new web-application from scratch in the basic JavaScript, HTML and CSS method removed any restriction on the design and functionality of the application. Highcharts was also used to create graphs and visualizations.

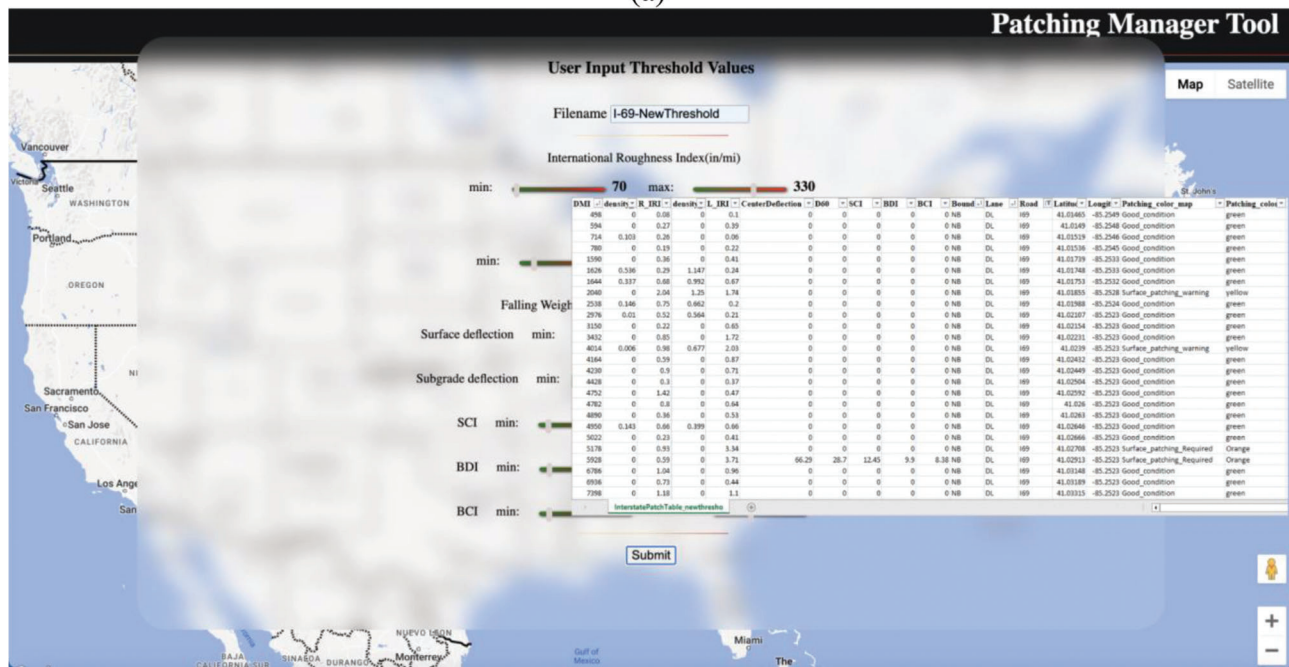
### 6.4.2 Google Maps, Street View

The Google API was used for mapping the points, due to its Street View feature. The Street View feature is fast and useful in surveying the roads virtually near an interesting PCA value to understand the cause leading to it. We had several times found high IRI values on downslopes, curves, turns or signals. These expected high IRI values should be excluded when using the IRI data. We used the ADA3 software and Google Street View extensively to ignore extremely high IRI values which occurred at expected features of roads in the patching algorithm. The Google API is free for 200 hits per day for the basic free account and was never paid for during the project.





(a)



(b)

**Figure 6.3** Web-based patching manager tool: (a) patching suggestion for the example road I-69 using color coded markers and graphs analyzing the parameters, and (b) user input threshold selector for patching suggestion calculation with an example patching table.

#### 6.4.3 Browser Compatibility and Time of Loading with Large Data on Map

The current version of PMT uses the Google chrome browser. It has not been tested for compatibility with other browsers, but it is not uncommon for application to work on all types of browsers.

Updating the PMT for compatibility with popular browsers isn't a difficult task.

#### 6.4.4 Protection and Security

The PMT uses basic HTTP server inside the Purdue university network but requires HTTPS server connec-

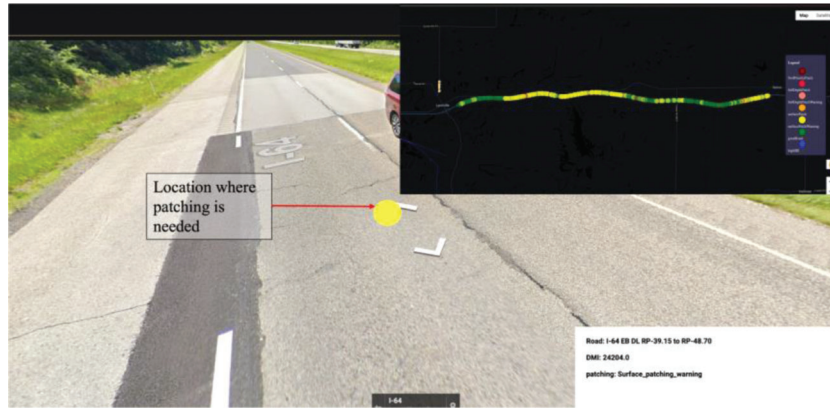


**Figure 6.4** Example of the final output of patching suggestion in PMT.

tion and CORS enabled settings when hosted on GitHub pages. We have also faced connection issues with other secure internet networks like the University of Reno, Nevada and INDOT. The application works fine in public networks.

## 7. INDOT IMPLEMENTATION

The open-source PMT tool is a powerful means of visualizing and interpreting PCA data. However, being hosted outside of the INDOT organization presents challenges for adoption and integration with INDOT's existing tools, namely ArcGIS and ArcGIS Online. To address these issues and enable INDOT engineers to utilize the research from this project, the core algorithm was deployed on top of a new strategy for data storage and visualization.

In summary, the raw data exported from various measurement devices and software are first processed by two separate Python scripts. The first script combines and re-aligns the disparate data files to a common reference. The second script applies the patching table algorithm from an external file containing pre-designed thresholds. Finally, feature manipulation engine (FME), a no-code data translation and transformation tool preferred by INDOT, is used to load the final data into both an INDOT-hosted Oracle database and an ArcGIS Online hosted feature layer.

Using ArcGIS Online, a dashboard was created as the primary research product; however, the feature layer can be directly used within any existing or new ArcGIS project. If new roads are collected or improved thresholds are determined, the entire dataset is easily re-processed and re-imported through the FME workflow, which intelligently updates existing data points while also adding new ones. The result is functionally similar to PMT but implemented within INDOT's preferred toolset.

### 7.1 Data Sources

The data source for the implementation was the same as that used for the algorithm development and PMT

itself. As a review, the data comes from two primary sources: WayLink and INDOT FWD datasets. Similar measurements collected from other instruments, such as pathways and traffic speed deflector (TSD), could easily be incorporated into the processing in the future.

For this work, IRI, CD, road surface images, and right-of-way (ROW) images were collected by the WayLink laser van. All roads have ROW imagery available; however, not all roads have been processed to include proper surface images. This processing requires a custom version of the WayLink ADA3 software, which at the time of this report is not yet installed on INDOT-managed computers.

FWD data is provided by INDOT research directly and is stored as an Excel worksheet. To simplify managing this worksheet, the user can provide a single workbook with all current FWD data in one sheet, and the processing scripts will correctly take only the data from the road of interest. In parallel, a separate project has been working to store all FWD data in the same Oracle database used by this project. A future work item could enhance the scripts to query the FWD data directly, removing the need for the user to manage the Excel worksheet at all.

### 7.2 Data Processing

There is a multi-step procedure to process the raw data into a patching table and final storage. The general flow is shown in Figure 7.1. First, WayLink 3D laser and image data is processed into IRI, crack density, and ROW and surface images using the ADA3 software. Second, the FWD and/or TSD measurement data is processed using the department's standard techniques for computing the various FWD metrics of interest. Data fusion and steps three and four are implemented by this work and are described in the remainder of this section.

#### 7.2.1 Python Script: *merge.py*

The first script, *merge.py*, loads all data and aligns them to one common DMI reference by fusing the datasets over GPS position data. This results in a set of

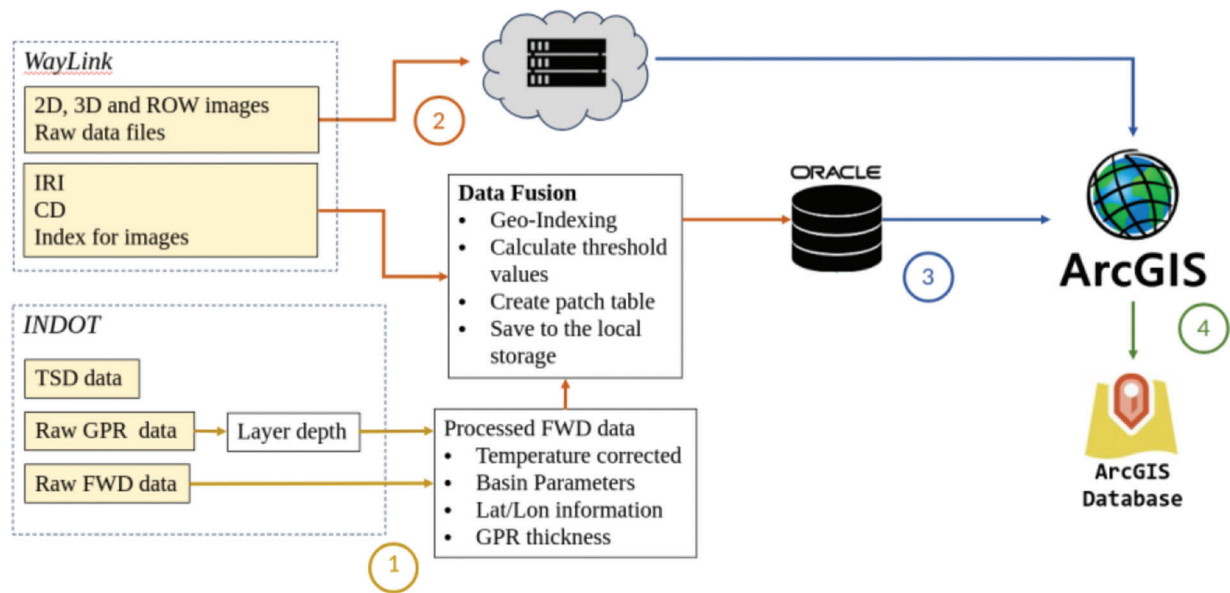


**Figure 7.1** Flowchart for processing raw measurement data through the SPR-4521 algorithm and into the INDOT preferred storage and visualization tools.

tidy CSV files, one per road, which includes all data of interest for each sample from all input data files. Each CSV represents one entire “scanning” project, which is generally limited to one road but may include scans of multiple lanes and directions within the same reference posts.

The help listing of merge.py is:

Usage: merge.py [OPTIONS] FWD WAYLINK...

This script merges FWD data (in excel format) with all WAYLINK exports

provided.

Options:

--baseUrl TEXT Based URL where images are served

-o, --output TEXT Path to write exported CSV. [required]

--help Show this message and exit.

The “FWD” parameter specifies the path to the Excel sheet containing the FWD data, and “WAYLINK” is the path to a Waylink export to be processed. Multiple Waylink paths may be provided to process more than one road and/or export at a time. The --baseUrl option allows changing the base URL used to construct weblinks to ROW and surface images. By default, this value is set to a web host at Purdue University, which currently contains most of the initial road’s imagery. It remains an open issue for INDOT to determine where the images could be stored more permanently. Finally, the -o option is required and should be set to the path where the output CSV files can be written.

An example instantiation of merge.py may look something like:

```
$ python merge.py ./FWD/FWD.xlsx ./Waylink/* -o
./merged-exports/
```

The WayLink folder contains the exports of multiple roads (as is typical for it’s export features) and all roads are to be processed.

#### 7.2.2 Python Script: spr4521.py

The second script, spr4521.py, loads both the output CSV from merge.py and an Excel sheet of thresholds and applies the SPR-4521 patching algorithm. The CSV files are amended in place to include the patching recommendation. If the algorithm or thresholds improve over time, the spr4521.py script can simply be run on the existing CSV files, and the patching recommendation will be updated in place. There is no need to re-run merge.py unless the underlying data has changed. Thresholds for each road type must be provided externally by the user, using the methods described in this report. Initial thresholds were proposed, but we expect that they will be refined as more data becomes available over time.

The help listing of spr4521.py is:

Usage: spr4521.py THRESHOLDS [EXPORTS]...

This script computes the SPR4521 patching recommendation for each of the

provided EXPORTS CSV files, using the thresholds defined in THRESHOLDS. The

result is written directly into each EXPORTS file.

Options:

--help Show this message and exit.

Where “THRESHOLDS” is the user-managed Excel workbook that includes the SPR4521 thresholds for each road type. “EXPORTS” is a list of merge.py output CSV files for computing the patching recom-



mendation. Multiple paths, or a path wildcard, can be included to process more than one export at a time. A CSV export can be directly re-processed by spr4521.py to update the patching recommendation if the threshold values are updated.

An example instantiation of merge.py may look something like:

```
$ python spr4521.py ./thresholds.xlsx ./merged-exports/*
```

The merged-exports folder contains the exports of multiple roads and all roads are to be processed.

### 7.2.3 Feature Manipulation Engine (FME): Oracle Database

The INDOT Oracle Database server is considered the permanent storage for patching recommendation data. To transfer the SPR-4521 exported CSV data to Oracle, a custom schema and FME workflow (shown in Figure 7.2) is used.

The Oracle database schema includes two separate tables. The first, SPR4521\_PATCHING\_PROJECT, stores all common metadata around a particular data collection over a specific road segment, lane, and travel direction. The second table, SPR4521\_PATCHING, stores the patching recommendation at each location and, for visualization purposes, the raw measurement data itself. Each row in this table can be joined back to a particular SPR4521\_PATCHING\_PROJECT entry to identify the collection activity that the data originated from.

In addition to storing the outputs in Oracle, the FME workflow has some additional functions. The first is to compute the starting and ending DMI values for each road segment, lane, and direction. While these values are not directly used in this work, they are extremely convenient when cross-referencing against other INDOT datasets, such as INDOT's own road lines. The second function is filtering the exports for locations with missing or invalid data. We filter these points from the data so that the database schema can remain restrictive about the data structure, which greatly simplifies the visualization tasks described later. The patch recommendation algorithm is not able to properly recommend a patch in these cases, so no actionable data is lost by culling it at this point.

Finally, the FME workflow compares the incoming data with data that already exists in the Oracle tables to determine which points only need to be updated and which are new additions. This results in an idempotent data loading flow that can be run as many times as needed with no adverse effects (other than updating the database when needed). Therefore, when a new road is added to the dataset, or when the recommendation thresholds are updated over time, the entire collection of existing CSV data can be re-processed in bulk by spr4521.py and trivially re-run through the same FME flowgraph. Locations with changed recommendations will be updated, new locations appended to the table, and data with no changes left unmodified.

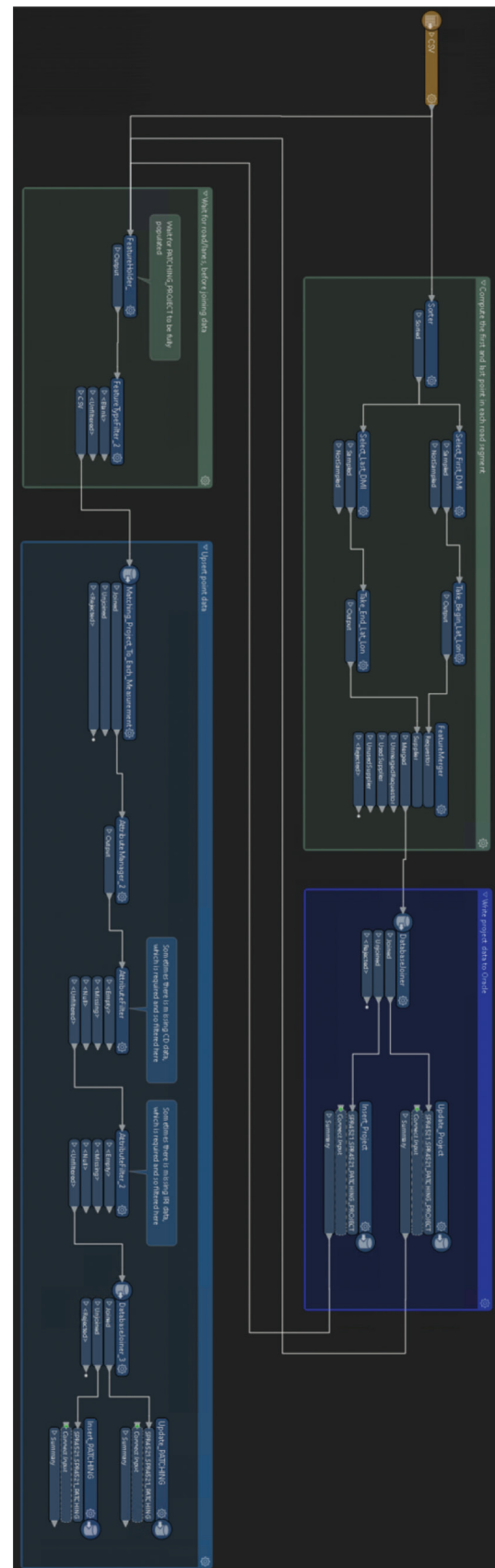


**Figure 7.2** FME workflow to load CSV output and load into Oracle (rotated).

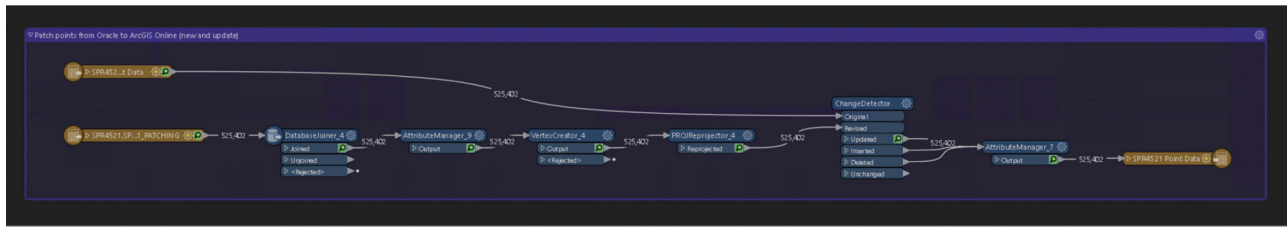


**Figure 7.3** FME workflow for transferring data stored in SPR-4521 Oracle tables into ArcGIS Online for visualization and custom analysis.

### 7.2.4 Feature Manipulation Engine (FME): ArcGIS Online

As the final step of the data processing pipeline, data from the permanent Oracle tables is transferred to an ArcGIS Online point-based hosted feature layer. This hosted feature can easily be included in any INDOT ArcGIS project for custom analysis or viewed through a project-developed dashboard. An FME workflow, shown in Figure 7.3, is also used for this step.

Simpler than the last workflow, this step downloads all data from the Oracle tables and the existing ArcGIS feature layer, compares the two to determine which data in ArcGIS needs to be updated, removed, or inserted. For the sake of nice visualizations, we update any record going into ArcGIS that does not have a ROW and/or surface image to link to an “Image Not Available” picture so that it is clear to the user that the data is not available, as opposed to the data layer having an error. Finally, the various updates, deletions, and additions are sent to ArcGIS via their web API, and the updated data is immediately available to consumers of the hosted feature layer. As with the first FME workflow, this workflow is also idempotent and can be run as often as desired with no adverse effects other than to push the ArcGIS feature layer to be synchronized with the current contents of the Oracle data tables.

### 7.3 ArcGIS Online Feature Layer

The flexibility that ArcGIS Online provides with hosted feature layers is the key feature that will enable the adoption of the data layers internally at INDOT. The feature layer can simply be shared with other INDOT users for them to drop into any existing or new ArcGIS project under development. Because the feature layer can carry styling and other metadata, it can be trivially added to a project with little to no customization by the user. ArcGIS feature layers are not just limited to ArcGIS Online; they can be downloaded and brought into an ArcGIS desktop project just as easily and still benefit from automatic updates when the feature layer itself is edited.

Figure 7.4 shows an example of the data layer added to a blank ArcGIS Online web map project. The symbology is already defined to show patching recommendations by color. Circles represent data without FWD, and triangles represent locations with FWD.

This is critical information because FWD data can only be collected at a relatively coarse rate compared to IRI, crack density, and rutting. Yet, it is the only measurement available that can indicate sub-surface issues. So, while the high-density sampling of the WayLink laser van is useful in understanding the state of the pavement, FWD data points provide context to the state of the sublayers in the area.

Selecting a data point of interest will cause a pop-up (shown on the left side of the map plot in Figure 7.4), which details the location and raw data used to determine the patching recommendation. Additionally, if available, the ROW and road surface imagery will be shown.

### 7.4 ArcGIS Dashboard

While the ArcGIS Online hosted feature layer is an invaluable resource, it may not be the most effective means of evaluating a particular road segment when developing patching requirements. As a result, the project also developed a dashboard product that the customer can use to more easily navigate through the data of a road segment, locate issue areas, and verify patching recommendations from charts of the raw data and ROW and surface images.

Figure 7.5 shows a nominal example of the SPR-4521 dashboard for a portion of the eastbound driving lane of I-64. The top row of the dashboard displays the ROW and surface images of the selected points. Below that is a zoomable and panable map, providing the context of the patching recommendations in the neighboring area. On the right is the detailed raw data of the currently selected point. Finally, at the bottom of the dashboard is a plot of the left and right IRI measurements along the entire length of the road. The metric plotted can be changed to any of the raw measurement variables.

The hosted feature layer contains all data collected and loaded, so there are many data points within the map and plots that may not be of interest for the user’s current use case. The filters on the left side of the screen can be used to filter and limit the display of both the map and plot widgets to just the road, lane, and/or direction of interest. This increases the performance of the dashboard itself and makes interpreting the plots considerably easier.

The metric plot on the bottom row of the dashboard can be used to filter and control the view of the map.

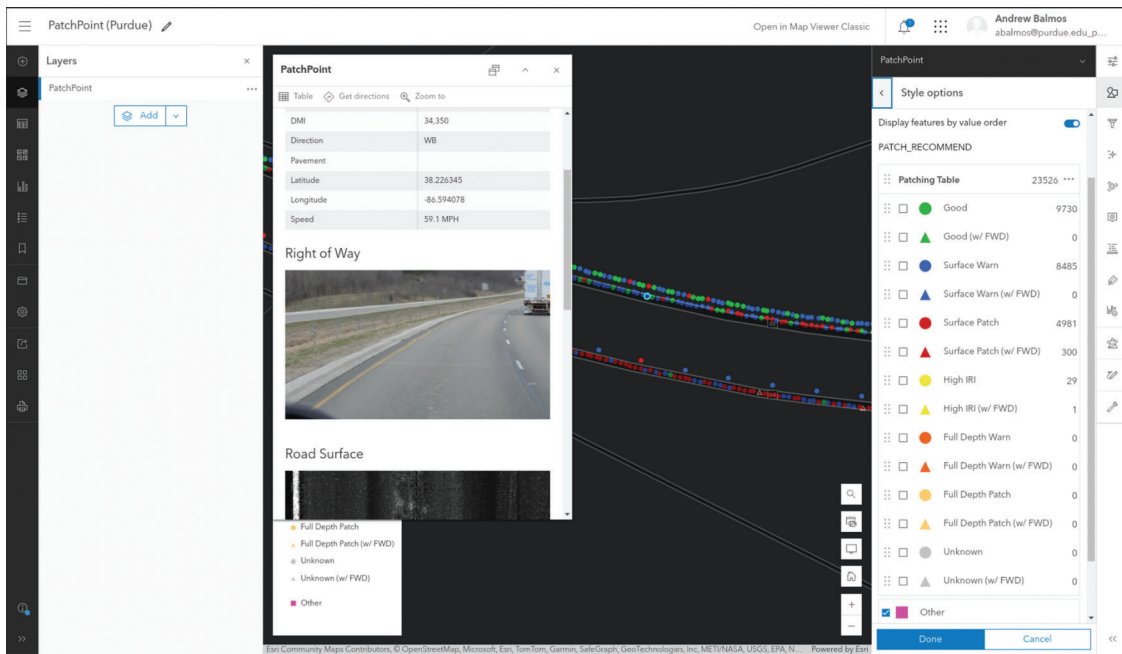


**Figure 7.4** Default styling of SPR-4521 patching recommendations layered into a new ArcGIS project.

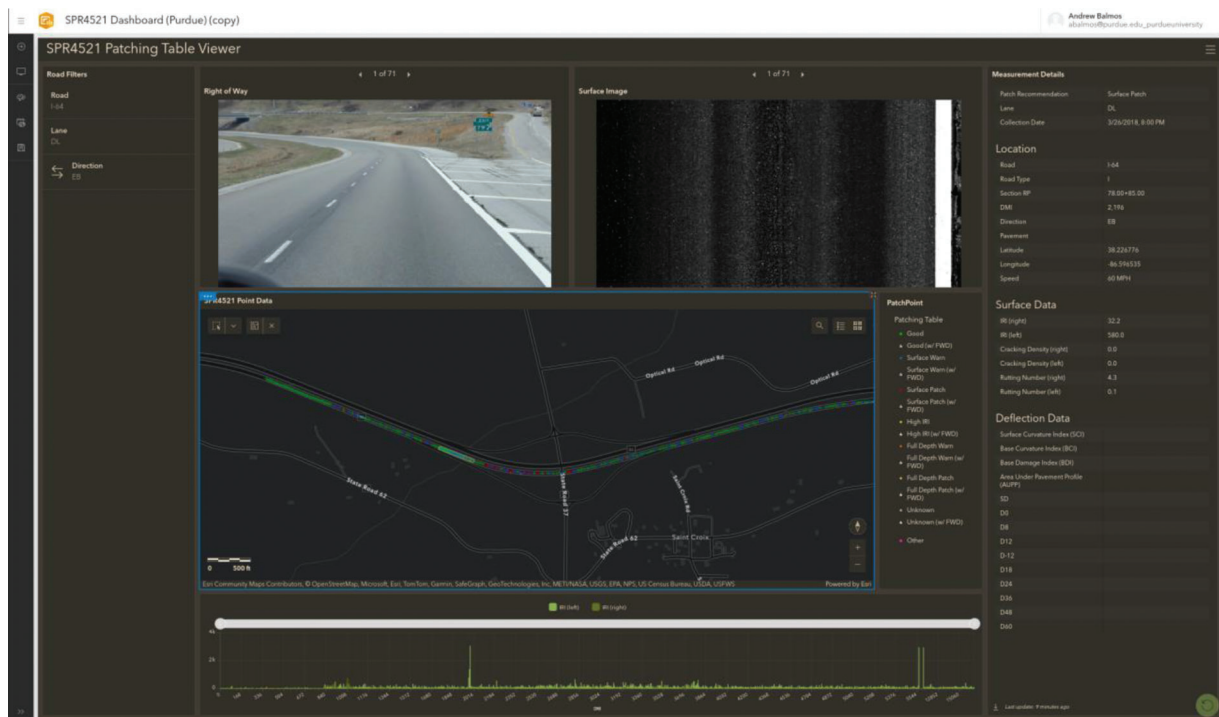


**Figure 7.5** ArcGIS Online dashboard for the SPR-4521 hosted feature layer, designed to enable a more effective review of a recommended patching table.

This enables a very powerful workflow where anomalies in a certain measurement series can be quickly “zoomed” into and verified or explained with the context of neighboring points and ROW and road surface images.

For example, in this case, there is a sudden jump in the average left IRI somewhere around 830 DMI. This

would not be a natural failure process for a continuous road of the same age, so it may be worth exploring what the cause might be. By click-and-drag selecting the area on the plot directly before and after the sudden rise, the map view will be filtered to show just the measurement points in that selected region, as shown in Figure 7.6.

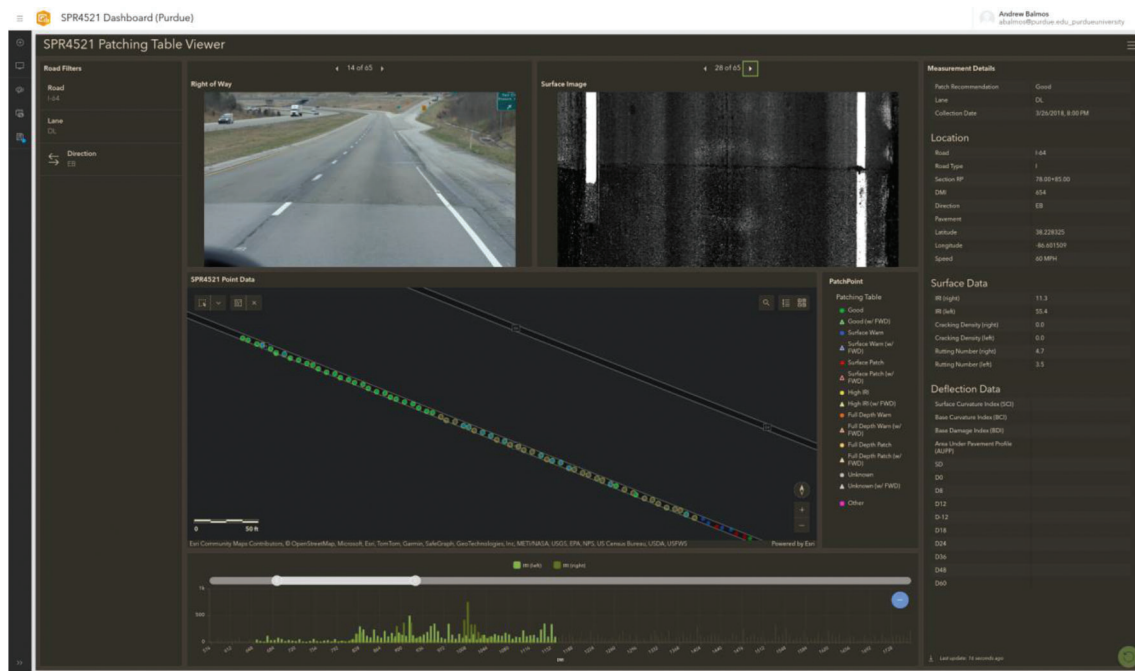


**Figure 7.6** Selecting points in the line graph visually filters the points in the map. This allows for quickly “zooming” into areas of interest based on abnormal measurement trends.



**Figure 7.7** By selecting a small number of locations of interest, one can “click through” the set of ROW and surface images to explain and/or validate patching recommendations. In this case, the sudden spike of IRI can be accounted for by noticing that the road transitions from new to old, formerly patched pavement.

By then selecting those points on the map and cycling through the ROW and surface images, it is quickly determined that the sudden rise can easily be accounted for by the pavement transitioning from new to older.

Similarly, a few DMI further down the road, as shown in Figure 7.7, the older portion of the road has previously been patched, accounting for the rather “spiky” IRI measurements in the older section.



## 8. FUTURE WORK

Socialization of the tool within INDOT, particularly the ArcGIS Online-based version of the software, is a key next step. The project is in a prime position to collect user feedback to either improve the visualizations to address common questions or refine the patching algorithm to reflect the needs of the engineering team.

Additionally, a traffic speed deflector (TSD) measurement device and data could greatly expand the size of the road network with automated patching recommendations in very little time. The human time needed to collect the underlying data is this work's primary constraint. Moreover, the larger dataset would allow for additional PCA parameters to improve the accuracy and further refine and validate the determined threshold values.

GPR data could also potentially increase the resolution of patching depth suggestions and improve sub-surface recommendations in general.

## 9. RESULTS SUMMARY AND RECOMMENDATIONS

### 9.1 Results Summary

This study proposes a reliability-SNR-based threshold calculation method for integrated PCA parameters. The data fusion approach integrating structural and functional assessment parameters with the matched geographical location describes the overall pavement assessment with better accuracy. It considers roughness, cracking and FWD deflections at the same location, allowing the automation of improved patching suggestions. The patching suggestion algorithm would incorporate the overall pavement condition information and could create five pavement condition ratings based on the distress level in three major layers of the pavement structure. The algorithm was tested using calculated PCA parameter threshold values for Interstate full-depth asphalt pavement segments. Comparative analysis of PCA parameters was able to detect localized distresses. It could reduce the bulk human resource and time required in a manual routine survey. The developed threshold-based patching suggestion algorithm was reinforced with a web-based application: PMT to assist in the current practices of PMS. The key features of the web based PMT application are summarized below.

- The web-application plots comprehensive patching suggestions with color-coded markers for a selected road segment on a map.
- PMT integrates two-dimensional road surface and ROW images to aid visual field assessments.
- PMT allows users to take advantage of Google Street View at the patching locations for 3D virtual spatial analysis.
- Histogram and scatter plots are included to analyze the distribution or pattern in PCA parameters along/among the selected roads.

- PMT supports the manual adjustment of threshold values for each PCA parameter in the patching suggestion algorithm. This feature creates flexibility for users to customize the patching tables, which are essential for analyzing and updating maintenance standards.

The PMT web-based application can provide high-resolution comprehensive patching suggestion with key features summarized above, and it was successfully verified with ROW images and Google Street View map. Furthermore, this study introduced the approach to determine appropriate threshold values based on local road conditions, and this approach can be used for roads in other states or countries. Consequently, the PMT web-based application, along with the proposed approach for threshold determination can be applied to any region with different road conditions.

To better incorporate these results into the INDOT organization, the data was stored in a centrally hosted Oracle database, and PMT features were reimplemented in ArcGIS Online. With essentially one-to-one feature equivalence, this allows INDOT engineers to enjoy the same workflow improvements created by the open-source PMT tool without creating friction within the existing tools that INDOT uses daily.

### 9.2 Recommendations

1. FWD, IRI, CD and GPR data should be collected simultaneously for the same section of the roads to create an overall pavement condition assessment.
2. Patching depth is an essential factor in patching suggestion and should be included in patching tables.
3. The pavement maintenance according to the current condition of roads should be used for planning corrective maintenance. The eCDF of pavement condition assessment parameters can be used to distinguish the pavement in worse conditions.
4. The threshold values for the PCA parameters for maintenance requirement should be calculated by comparing the extent of deterioration of road sections and economic constraint on maintenance operations. It should be limited by the number of road sections that can be repaired in the current budget and be selected from the road sections in worst condition.
5. INDOT should socialize the ArcGIS Online-based version of the PMT to allow for proper user feedback in future work.

## REFERENCES

- AASHTO. (1993). *AASHTO guide for design of pavement structures*. American Association of State Highway and Transportation Officials.
- AASHTO. (2020). *Mechanistic-empirical pavement design guide: A manual of practice* (Third edition). American Association of State Highway and Transportation Officials.
- Abd El-Raof, H. S., Abd El-Hakim, R. T., El-Badawy, S. M., & Afify, H. A. (2018). Structural number prediction for flexible pavements using the long term pavement performance data. *International Journal of Pavement Engineering*, 21(7), 841–855.

- Anderson, D. A., & Thomas, H. R. (1984). Pothole repair in Pennsylvania. *Proceedings of Road School Purdue University* (p. 28–46).
- Baladi, G. Y., Prohaska, M., Thomas, K., Dawson T., & Musunuru, G. (2017). *Pavement performance measures and forecasting and the effects of maintenance and rehabilitation strategy on treatment effectiveness* (Publication No. FHWA-HRT-17-095). Federal Highway Administration.
- Bautista, F. E., & Basheer, I. (2008). *Jointed plain concrete pavement (JPCP) preservation and rehabilitation design guide*. California Department of Transportation.
- Bryce, J., Boadi, R., & Groeger, J. (2019). Relating pavement condition index and present serviceability rating for asphalt-surfaced pavements. *Transportation Research Record*, 2673(3), 308–312. <https://doi.org/10.1177/0361198119833671>
- Chang, C., Saenz, D., Nazarian, S., Abdallah, I. N., Wimsatt, A., Freeman, T., & Fernando, E. G. (2014). *TXDOT guidelines to assign PMIS treatment levels* (Report No. FHWA/TX-14/0-6673-P1). Center for Transportation Infrastructure Systems.
- Chikezie, C. U., Olowosulu, A. T., & Abejide, O. S. (2013). Multiobjective optimization for pavement maintenance and rehabilitation programming using genetic algorithms. *Archives of Applied Science Research*, 5(4), 76–83.
- Crook, A. L., Montgomery, S. R., & Guthrie, W. S. (2012). Use of falling weight deflectometer data for network-level flexible pavement management. *Transportation Research Record*, 2304(1), 75–85. <https://doi.org/10.3141/2304-09>
- Dong, Q., Huang, B., & Zhao, S. (2013). Field and laboratory evaluation of winter season pavement pothole patching materials. *International Journal of Pavement Engineering*, 15(4), 279–289. <https://doi.org/10.1080/10298436.2013.814772>
- FHWA. (2022). *State highway reliability report–Indiana* [Webpage]. U.S. Department of Transportation Federal Highway Administration. Retrieved November 20, 2022, from <https://www.fhwa.dot.gov/tpm/reporting/state/reliability.cfm?state=Indiana>
- Flora, W. F., Ong, G. P., & Sinha, K. C. (2010). *Development of a structural index as an integral part of the overall pavement quality in the INDOT PMS* (Joint Transportation Research Program Publication FHWA/IN/JTRP-2010/11). West Lafayette, IN: Purdue University. <https://doi.org/10.5703/1288284314261>
- Gkyrtis, K., Loizos, A., & Plati, C. (2021). *Integrating pavement sensing data for pavement condition evaluation*. *Sensors*, 21(9), 3104. <https://doi.org/10.3390/s21093104>
- Haider, S. W., Chatti, K., Baladi, G. Y., & Sivanewaran, N. (2011). Impact of pavement monitoring frequency on pavement management system decisions. *Transportation Research Record*, 2225(1), 43–55. <https://doi.org/10.3141/2225-06>
- Horak, E., Hefer, A., Emery, S., & Maina, J. (2015). Flexible road pavement structural condition benchmark methodology incorporating structural condition indices derived from Falling Weight Deflectometer deflection bowls. *Journal of Civil Engineering and Construction*, 4(1), 1–14.
- Ismail, N., Ismail, A., & Atiq, R. (2009). An overview of expert systems in pavement management. *European Journal of Scientific Research*, 30(1), 99–1119.
- Johnson, A. M. (2000). *Best practices handbook on asphalt pavement maintenance*. Minnesota Technology Transfer/LTAP Program, Center for Transportation Studies. <https://hdl.handle.net/11299/199769>
- Kavussi, A., Abbasghorbani, M., Nejad, F. M., & Ziksari, A. B. (2017). A new method to determine maintenance and repair activities at network-level pavement management using falling weight deflectometer. *Journal of Civil Engineering and Management*, 23(3), 338–346.
- Kim, M. Y., Kim, D. Y., & Murphy, M. R. (2013). Improved method for evaluating the pavement structural number with falling weight deflectometer deflections. *Transportation Research Record*, 2366(1), 120–126.
- Kulkarni, R. B., & Miller, R. W. (2003). Pavement management systems: Past, present, and future. *Transportation Research Record*, 1853(1), 65–71.
- Lee, J., & Shields, T. (2010). *Treatment guidelines for pavement preservation* (Joint Transportation Research Program Publication No. FHWA/IN/JTRP-2010/01). West Lafayette, IN: Purdue University. <https://doi.org/10.5703/1288284314270>
- Lytton, R. L. (1989). *Backcalculation of pavement layer properties*. ASTM International. <https://doi.org/10.1520/STP19797S>
- Maher, A., Gucunski, N., Yanko, W., & Petsi, F. (2001). *Evaluation of pothole patching materials* (Report No. FHWA NJ 2001-02). New Jersey Department of Transportation.
- McDaniel, R. S. (2020). *Best practices for patching composite pavements* (Joint Transportation Research Program Publication No. FHWA/IN/JTRP-2020/05). West Lafayette, IN: Purdue University. <https://doi.org/10.5703/1288284317116>
- McDaniel, R. S., Olek, J., Magee, B. J., Behnood, A., & Pollock, R. (2014). *Pavement patching practices—A synthesis of highway practice* (NCHRP Synthesis 463). National Cooperative Highway Research Program.
- Park, B., Cho, S., Rahbar-Rastegar, R., Nantung, T. E., & Haddock, J. E. (2022). Prediction of critical responses in full-depth asphalt pavements using the falling weight deflectometer deflection basin parameters. *Construction and Building Materials*, 318, 126019.
- Rada, G. R., Perera, R. W., Prabhakar, V. C., & Wiser, L. J. (2012). Relating ride quality and structural adequacy for pavement rehabilitation and management decisions. *Transportation Research Record*, 2304(1), 28–36.
- Rohde, G. T. (1994). Determining pavement structural number from FWD testing. *Transportation Research Record*, 1448, 61–68.
- Setiaputri, H. A., Isradi, M., Rifai, A. I., Mufhidin, A., & Prasetyo, J. (2020). Analysis of urban road damage with pavement condition index (PCI) and surface distress index (SDI) methods. *ADRI International Journal of Sciences, Engineering and Technology*, 6(1), 10–19.
- Sidess, A., Ravina, A., & Oged, E. (2021). A model for predicting the deterioration of the pavement condition index. *International Journal of Pavement Engineering*, 22(13), 1625–1636.
- Sollazzo, G., Fwa, T. F., & Bosurgi, G. (2017). An ANN model to correlate roughness and structural performance in asphalt pavements. *Construction and Building Materials*, 134, 684–693.
- Wang, K. C. P., Hou, Z., & Williams, S. (2011). Precision test of cracking surveys with the automated distress analyzer. *Journal of Transportation Engineering*, 137(8), 571–579.
- Wilson, T. P., & Romine, A. R. (2001). *Materials and procedures for repair of potholes in asphalt-surfaced pavements—manual of practice* (Report No. FHWA-RD-99-168). Federal Highway Administration.
- Wolters, A. S., & Zimmerman, K. A. (2010). *Current practices in pavement performance modeling* (Report No. FHWA-

- PA-2010-007-080307). Pennsylvania Department of Transportation.
- Xiao, M., Luo, R., & Yu, X. (2022). Assessment of asphalt pavement overall performance condition using functional indexes and FWD deflection basin parameters. *Construction and Building Materials*, 341, 127872.
- Zhang, A., Wang, K. C. P., Li, B., Yang, E., Dai, X., Peng, Y., Fei, Y., Liu, Y., Li, J. Q., & Chen, C. (2017). Automated pixel-level pavement crack detection on 3D asphalt surfaces using a deep-learning network. *Computer-Aided Civil and Infrastructure Engineering*, 32(10), 805–19.
- Zhang, Z., Claros, G., Manuel, L., & Damnjanovic, I. (2003). Development of structural condition index to support pavement maintenance and rehabilitation decisions at network level. *Transportation Research Record*, 1827(1), 10–7.

## APPENDICES

### **Appendix A. Processing of Raw 3D Laser Data in Waylink's ADA3 Software**



## APPENDIX A. PROCESSING OF RAW 3D LASER DATA IN WAYLINK'S ADA3 SOFTWARE

IRI and CD can be processed in the ADA3 software by single lane or by batches of lanes.

### **Single Lane Processing**

Use the open folder from file tab in the ADA3 software. Navigate to the .mdx file in the selected lane folder, select this file and click open. The ADA3 software populates the ROW image, 3D road surface image and 2D road surface image in three separate windows within the software screen by default.

## About the Joint Transportation Research Program (JTRP)

On March 11, 1937, the Indiana Legislature passed an act which authorized the Indiana State Highway Commission to cooperate with and assist Purdue University in developing the best methods of improving and maintaining the highways of the state and the respective counties thereof. That collaborative effort was called the Joint Highway Research Project (JHRP). In 1997 the collaborative venture was renamed as the Joint Transportation Research Program (JTRP) to reflect the state and national efforts to integrate the management and operation of various transportation modes.

The first studies of JHRP were concerned with Test Road No. 1 — evaluation of the weathering characteristics of stabilized materials. After World War II, the JHRP program grew substantially and was regularly producing technical reports. Over 1,600 technical reports are now available, published as part of the JHRP and subsequently JTRP collaborative venture between Purdue University and what is now the Indiana Department of Transportation.

Free online access to all reports is provided through a unique collaboration between JTRP and Purdue Libraries. These are available at <http://docs.lib.purdue.edu/jtrp>.

Further information about JTRP and its current research program is available at <http://www.purdue.edu/jtrp>.

## About This Report

An open access version of this publication is available online. See the URL in the citation below.

Jha, S., Zhang, Y., Bagchi, T., Balmos, A., Park, B., Haddock, J. E., Cho, S., & Krogmeier, J. V. (2024). *Comprehensive pavement patching tools and web-based software for pavement condition assessment and visualization* (Joint Transportation Research Program Publication No. FHWA/IN/JTRP-2024/29). West Lafayette, IN: Purdue University. <https://doi.org/10.5703/1288284317770>